

---


Electronic Theses and Dissertations, 2004-2019

---

2008

## The Endocytic Protein Numb Regulates App Metabolism And Notch Signaling: Implications For Alzheimer's Disease

George Kyriazis  
*University of Central Florida*

 Part of the [Microbiology Commons](#), [Molecular and Cellular Neuroscience Commons](#), and the [Molecular Biology Commons](#)

Find similar works at: <https://stars.library.ucf.edu/etd>

University of Central Florida Libraries <http://library.ucf.edu>

This Doctoral Dissertation (Open Access) is brought to you for free and open access by STARS. It has been accepted for inclusion in Electronic Theses and Dissertations, 2004-2019 by an authorized administrator of STARS. For more information, please contact [STARS@ucf.edu](mailto:STARS@ucf.edu).

---

### STARS Citation

Kyriazis, George, "The Endocytic Protein Numb Regulates App Metabolism And Notch Signaling: Implications For Alzheimer's Disease" (2008). *Electronic Theses and Dissertations, 2004-2019*. 3461. <https://stars.library.ucf.edu/etd/3461>

**THE ENDOCYTIC PROTEIN NUMB REGULATES APP METABOLISM  
AND NOTCH SIGNALING: IMPLICATIONS FOR ALZHEIMER'S  
DISEASE**

by

GEORGE A. KYRIAZIS  
B.S. University of Athens, 1994  
M.A. University of Central Florida, 2005

A dissertation submitted in partial fulfillment of the requirements  
for the degree of Doctor of Philosophy  
in the Burnett School of Biomedical Sciences  
in the College of Medicine  
at the University of Central Florida,  
Orlando, Florida

Summer term  
2008

Major Professor: Sic L. Chan

© 2008 George A. Kyriazis

## ABSTRACT

Increased production of neurotoxic forms of amyloid  $\beta$  ( $A\beta$ ) peptide via altered proteolytic cleavage from its precursor, the amyloid protein precursor (APP), and abnormalities in neuronal calcium homeostasis play central roles in the pathogenesis of Alzheimer's disease (AD). Notch1, a membrane receptor that controls cell fate decisions during development of the nervous system, has been linked to AD because it is a substrate for the  $\gamma$ -secretase enzyme activity that involves the presenilin-1 protein in which mutations cause early-onset inherited AD.

Numb is an evolutionarily conserved endocytic adapter involved in the internalization of transmembrane receptors. Mammals produce four Numb isoforms that differ in two functional domains, a phosphotyrosine-binding domain (PTB) and a proline-rich region (PRR). Expression of these alternative spliced Numb transcripts is tightly regulated both temporally and spatially during development and aberrant Numb isoform expression has been associated with increased risk for cancers. Recent studies showed that the PTB domain of Numb interacts with the cytoplasmic tails of APP and Notch but the functional relevance of these interactions with respect to AD pathogenesis is not clear. In the current study, we proposed to investigate the biological consequences of the interaction of the Numb proteins with APP and Notch in neural cells stably overexpressing each of the four human Numb proteins.

Converging lines of evidence indicate that the endocytic pathway is involved in the aberrant processing of APP. Yet little is known about the underlying regulatory mechanism of APP endocytosis and trafficking. Elucidating the functional consequences of the interaction of APP with the Numb endocytic adapter proteins will provide a better understanding of the underlying mechanisms of aberrant APP processing. In the first part of our studies, we found that expression of the Numb isoforms lacking the insert in the PTB (SPTB-Numb) caused the

abnormal accumulation of cellular APP in the early endosomes, and increased the levels of C-terminal APP fragments and A $\beta$ . By contrast, expression of the Numb isoforms with the insert in PTB (LPTB-Numb) leads to the depletion of cellular APP and coincides with significantly lower production of APP derivatives and A $\beta$ . The contrasting effects of the Numb isoforms on APP metabolism appeared to be independent of the composition of the PRR domain and were not attributed to differences in the expression of APP nor the activities of the various APP-processing secretases.

Evidence is emerging that Notch signaling plays a role in the regulation of apoptosis in neural progenitors and in post-mitotic neurons. Numb has been shown to suppress Notch signaling by enhancing endocytosis and degradation of the Notch receptor. Whether the aberrant expression of the Numb isoforms leads to aberrant Notch signaling, and how this might promote neuronal degeneration is still not known. In the second part of our studies, we found that expression of SPTB-Numb protein enhances neuronal vulnerability to serum deprivation-induced cell death by a mechanism involving the dysregulation of cellular calcium homeostasis. Neural cells expressing SPTB-Numb exhibited markedly higher protein levels of transient receptor potential canonical 6 (TRPC6) channels and increased calcium entry in response to store depletion. These effects are mediated by Notch1 as pharmacological inhibition of Notch1 abrogated TRPC6 upregulation. We also found that serum deprivation increased TRPC6 upregulation by a mechanism dependent on Notch activation. Knockdown of TRPC6 expression stabilized intracellular calcium homeostasis and significantly suppressed serum deprivation-induced death suggesting that Notch-dependent TRPC6 upregulation contributes in part to serum-deprivation induced death. Interestingly, expression of LPTB-Numb protein suppressed serum deprivation-induced activation of Notch and the subsequent upregulation of TRPC6 and

cell death. The latter finding further strengthens the link between the Numb isoform specific effect on Notch activation and the Notch-dependent upregulation of TRPC6. Finally, we showed that the Numb proteins differentially impact Notch activation by altering the endocytic trafficking and processing of Notch. Taken together, these studies demonstrate that aberrant expression of the Numb proteins may influence APP metabolism and Notch-mediated cellular responses to injury by altering their endocytic trafficking and processing.

Dedicated to

**Sisyphus**

The eternal human hero who courageously carries out his absurd sentence, clandestinely knowing he is free as the rock rolls down the mountain.

## TABLE OF CONTENTS

LIST OF FIGURES .....	x
LIST OF TABLES .....	xii
CHAPTER I Numb endocytic adapter proteins regulate the transport and processing of the amyloid precursor protein in an isoform-dependent manner: Implications for Alzheimer's disease pathogenesis.....	1
Introduction.....	1
Materials and Methods.....	6
Antibodies and reagents .....	6
cDNA Constructs .....	7
Cell lines and transfections .....	7
Treatments.....	8
RNA isolation and PCR.....	8
SDS-PAGE and Western blotting.....	9
Immunofluorescence microscopy .....	9
Measurements of sAPP levels.....	10
A $\beta$ 40/42 sandwich enzyme-linked immuno-sorbent assay (ELISA) assay .....	10
Measurements of secretase activity .....	11
Cell surface biotinylation.....	11
Results.....	12
Expression of Numb proteins alters APP metabolism in a manner dependent upon the PTB domain.....	12
Expression of Numb proteins alters A $\beta$ generation in a manner dependent upon the PTB domain.....	13
Expression of the Numb proteins does not affect the level of APP expression nor the proteolytic activities of the APP processing secretases.....	16



The effects of Numb on APP metabolism is dependent on its interaction with APP and the internalization of APP .....	18
Numb proteins influence the endosomal trafficking of APP .....	18
Effect of the Numb proteins on the endosomal sorting of APP to the recycling pathway ...	22
Effects of the Numb proteins on the endosomal sorting of APP to the degradative pathway .....	24
The proteasome-mediated degradative pathway is not involved in the regulation of APP metabolism by the Numb proteins .....	26
Expression of Numb proteins alters the levels of the Rab family of endocytic regulators...	29
Stress induces the selective upregulation of SPTB-Numb transcripts .....	30
Discussion .....	32
CHAPTER II Effects of Numb isoforms on Notch-dependent upregulation of TRPC6 calcium channels .....	38
Introduction .....	38
Materials and methods .....	44
Antibodies and reagents .....	44
Cell culture and treatments .....	44
Intracellular calcium measurements .....	45
Cell death assays .....	46
siRNA .....	47
RNA isolation and Real-Time PCR .....	47
Results .....	49
SPTB-Numb is characterized by SOCE and increased expression of TRPC calcium channels .....	49
Serum deprivation-induced cell death is mediated by TRPC6 upregulation .....	51
Notch signaling is enhanced in SPTB-Numb .....	55
Serum deprivation increases Notch signaling in PC12 cells .....	57

Suppression of Notch signaling by a $\gamma$ -secretase inhibitor attenuates TRPC6 expression in SPTB-Numb.....	59
Jagged1- mediated activation of Notch induces TRPC6 upregulation in PC12 cells.....	62
Increased levels of TRPC6 channels account for the enhanced SOCE in SPTB-Numb .....	63
Discussion.....	68
REFERENCES.....	74

## LIST OF FIGURES

Figure 1. APP processing and amyloid $\beta$ peptide ( $A\beta$ ) deposition .....	1
Figure 2. Sub-cellular localization of APP processing .....	2
Figure 3. Numb isoforms and their structural domains .....	4
Figure 4. Isoform specificity in the processing of APP and generation of $A\beta$ by the Numb proteins.....	14
Figure 5. Lack of isoform specificity on the expression of APP and the activities of the APP secretases.....	17
Figure 6. Isoform specificity of Numb effects on APP metabolism is dependent on the interaction of the Numb proteins with APP and its subsequent internalization.....	20
Figure 7. Effect of the Numb proteins on the sorting of APP to the recycling pathway .....	23
Figure 8. Effect of the Numb proteins on the sorting of APP to the degradative pathway .....	27
Figure 9. Effect of the Numb proteins on the levels of small Rab GTPases .....	30
Figure 10. Detection of alternatively spliced Numb transcripts under normal and stressed conditions.....	31
Figure 11. Schematic diagram: Numb isoform-specific regulation of APP trafficking and $A\beta$ generation.....	37
Figure 12. Notch signaling activation.....	41
Figure 13. Thapsigargin-induced SOCE and TRPC calcium channel expression.....	50
Figure 14. TRPC6 upregulation mediates serum deprivation-induced cell death in PC12 cells via a mechanism that involves the SPTB isoform of Numb.....	54
Figure 15. Notch signaling is enhanced in SPTB-Numb.....	56

Figure 16. Serum deprivation increases Notch signaling in PC12 cells .....	59
Figure 17. Notch inhibition abrogates TRPC6 upregulation in SPTB-Numb .....	61
Figure 18. Notch activation induces the expression of TRPC6 in PC12 cells.....	63
Figure 19. TRPC6 upregulation mediates the enhanced SOCE in SPTB-Numb .....	66
Figure 20. Schematic diagram: SPTB-Numb affect the Notch-dependent upregulation of TRPC6 calcium channels.....	72

## **LIST OF TABLES**

Table 1. Oligonucleotide sequences of primers used for Real Time RT-PCR .....	48
---	----

# CHAPTER I

## NUMB ENDOCYTIC ADAPTER PROTEINS REGULATE THE TRANSPORT AND PROCESSING OF THE AMYLOID PRECURSOR PROTEIN IN AN ISOFORM-DEPENDENT MANNER: IMPLICATIONS FOR ALZHEIMER'S DISEASE PATHOGENESIS

### *Introduction*

The amyloid precursor protein (APP) is an integral transmembrane glycoprotein which is highly expressed in the brain and plays an important role in neuronal function <sup>1</sup>. The abnormal processing of APP to generate the amyloid  $\beta$ -peptide ( $A\beta$ ) leads to the extracellular neuritic plaques characteristic of Alzheimer's disease (AD) <sup>1-3</sup> (**Fig. 1**). The rate of  $A\beta$  production is believed to be a key determinant of the onset and progression of AD. While proteolytic processing of APP and characterization of the APP-cleaving enzymes ( $\alpha$ -,  $\beta$ - and  $\gamma$ -secretases) have revealed important targets for drug discovery, the regulation of APP trafficking is less well understood.

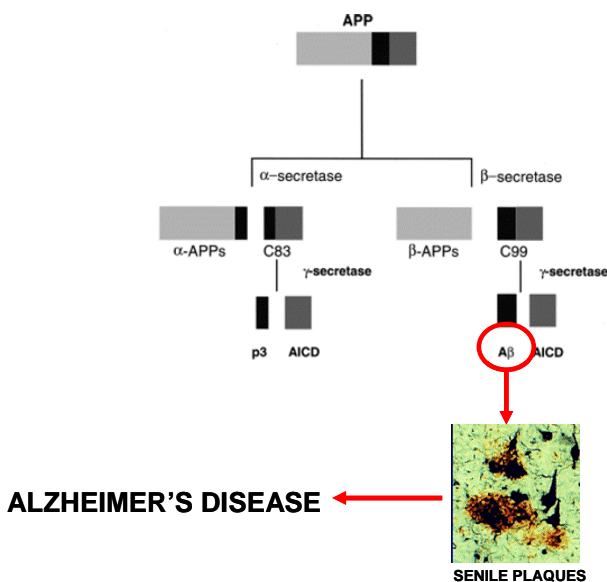


**Figure 1. APP processing and amyloid  $\beta$  peptide ( $A\beta$ ) deposition**

Several recent findings support the idea that the intracellular transport and subcellular localization of APP are crucial determinants of APP processing and A $\beta$  generation.<sup>4, 5</sup> One pathway for A $\beta$  generation involves the re-internalization of membrane-bound full length APP<sup>4, 5</sup>. Endosomes have been shown to be intracellular compartments where the sequential action of  $\beta$ - and  $\gamma$ -secretases generates amyloidogenic C-terminal fragments of APP (APP-CTFs) and A $\beta$ <sup>1-3</sup>. APP is also targeted to, and degraded in, the lysosomes<sup>6</sup>. On the other hand, cleavage within the A $\beta$  region of APP by  $\alpha$ -secretase, which prevents the production of A $\beta$ , occurs in a late compartment of the secretory pathway such as the Golgi or at the cell surface<sup>7</sup> (**Fig. 2**). Deletion of the APP cytoplasmic tail or inhibition of endocytosis has been shown to reduce A $\beta$  levels suggesting that endocytosis is critical for A $\beta$  generation<sup>4, 5, 8</sup>. Understanding the mechanisms that regulate APP trafficking to distinct subcellular compartments with the different secretase activities is important for developing strategies to reduce abnormal processing and to prevent A $\beta$ -induced neurotoxicity.

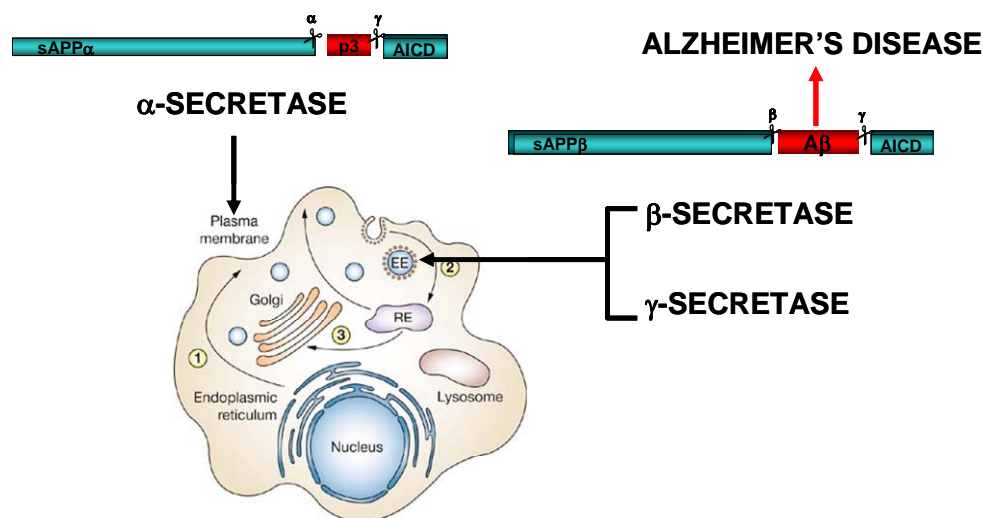
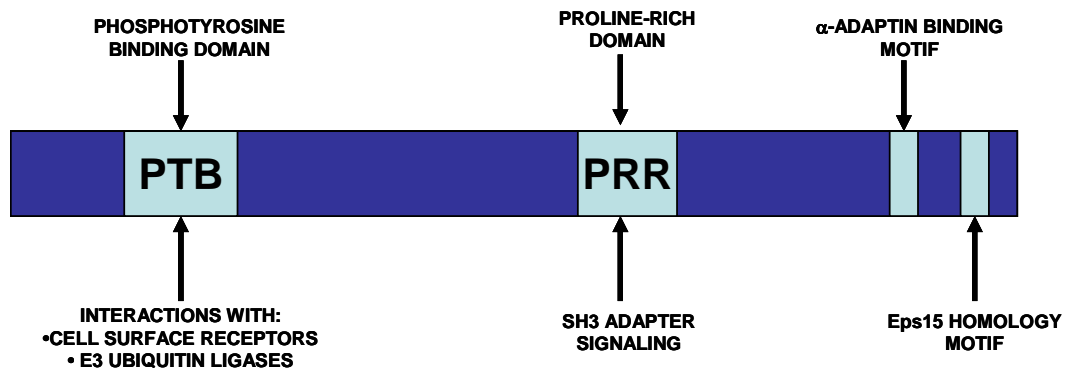


**Figure 2. Sub-cellular localization of APP processing**

Numb is an evolutionarily conserved protein identified by its ability to control cell fate in the nervous system of *Drosophila*<sup>9, 10</sup>. Numb contains two protein-protein interaction domains, a phosphotyrosine-binding (PTB) domain and a proline-rich region (PRR) that functions as an SH3-binding domain<sup>11, 12</sup>. Whereas only one form of Numb has been identified in *Drosophila*, mammals produce four alternatively spliced variants of Numb that differ in the length of their PTB (lacking or containing an 11 amino acid insert) and PRR (lacking or containing a 48 amino acid insert) domains<sup>11, 12</sup>. All Numb proteins contain the NPF (asparagine-proline-phenylalanine) and DPF (aspartate-proline-phenylalanine) motifs that are critical for interaction with proteins containing the Eps15 Homology (EH) domain and with the clathrin protein AP-2, respectively (**Fig. 3**). Numb can associate with clathrin-coated pits, vesicles and endosomes, suggesting it functions as an endocytic adapter protein<sup>13, 14</sup>. Numb plays a role in the internalization of receptors that are not only involved in cell-fate decisions during CNS development<sup>15</sup>, but also in neuronal maturation, differentiation and survival<sup>16, 17</sup>. Notch is an evolutionary conserved transmembrane receptor that specifies cell fate in a wide variety of tissues and organisms through local cell-cell interaction<sup>18</sup>. Numb regulates the endocytic and ubiquitin-dependent processing of Notch<sup>19</sup> and consequently the cell fate decisions determined by Notch signaling<sup>20, 21</sup>. In maturing neurons, Numb binds to the neural adhesion protein L1 and integrin in axonal growth cones and promotes their recycling<sup>22, 23</sup>.





Human Numb	Structure	Composition	MW (Kd)
	11 aa insert      48 aa insert		
Isoform 1		LPTB/LPRR	72
Isoform 2		LPTB/SPRR	66
Isoform 3		SPTB/LPRR	71
Isoform 4		SPTB/SPRR	65

**Figure 3. Numb isoforms and their structural domains**

Previous work has demonstrated an interaction between APP and Numb in mouse brain lysates and in cell culture<sup>24</sup>. Truncation and site-directed mutagenesis studies have shown that Numb binds to the YENPTY motif within the intracellular domain of APP<sup>24</sup>. Several other APP binding partners that interact with this motif including X11, Fe65, mDab, C-Abl and JIP-1 have been demonstrated to affect endogenous APP localization and processing<sup>25</sup>. Considering that Numb is an endocytic adapter protein, we determined whether expression of Numb influences the trafficking and processing of APP. Our results show that expression of Numb isoforms lacking the insert in the PTB (short PTB- or SPTB-Numb) caused the abnormal accumulation of cellular APP in the early endosomes and increased the levels of C-terminal APP fragments (APP-CTFs). By contrast, expression of the Numb isoforms with the insert in PTB (long PTB- or LPTB-Numb) causes a significant reduction in the cellular content of APP and APP-CTFs.

Interestingly, when cultured primary cortical neurons were subjected to trophic factor deprivation, the expression of the SPTB-Numb increased at the expense of LPTB-Numb, suggesting that pathophysiological conditions can alter Numb isoform expression in a manner that increases amyloidogenic processing of APP. Understanding the function of Numb in the trafficking of APP may provide insights into the regulation of APP processing in AD pathogenesis and lead to possible AD therapies.

## ***Materials and Methods***

### ***Antibodies and reagents***

Antibodies used for immunodetection of APP were 6E10 (anti-A $\beta$  1-17) and 22C11 (anti-sAPP $\alpha$ ) (Chemicon); anti-amino terminus of APP (2.F2.19B4, Chemicon), anti-carboxyl terminus of APP (APP643-695) and 4G8 anti-A $\beta$  (17-24) (Signet). The polyclonal antibodies to Numb were obtained from Santa Cruz (sc-15590) or Upstate (anti-pan-Numb). The antibodies to Rab proteins were: Rab5a (Santa Cruz), Rab4a (Santa Cruz), Rab11 (Santa Cruz) and Rab7 (Sigma). LAMP-1 antibody was from Santa Cruz. Antibodies to the following tags were: GST (glutathione S-transferase; Cell Signaling), HA epitope (Santa Cruz) and Flag epitope (Cell Signaling). Other antibodies included: ERK1/2 and phospho-ERK1/2, (Cell Signaling), dynamin1 (BD Biosciences), actin (Sigma), ubiquitin (Santa Cruz, P4D1), transferrin receptor (Zymed),  $\beta$ -secretase 1 (BACE 1; Sigma), presenilin-1 (PS1; Chemicon), nicastrin (Sigma), Aph-1 (Sigma), and Pen-2 (Santa Cruz). Immunofluorescence-conjugated secondary antibodies (Alexa Fluor 488-conjugated goat anti-mouse and Alexa Fluor 594-conjugated rabbit anti-goat IgG) were obtained from Molecular Probes. Additional reagents included: Lipofectamine Plus reagent (Invitrogen), FuGENE-6 (Roche), EZ-Link Sulfo-NHS-LC-Biotin (Pierce), DAPT (Calbiochem), lactacystin, peptide aldehyde N-carbobenzoxyl-L-leucinyll-leucinyll-leucinal (MG-132), chloroquine (Calbiochem) and NH<sub>4</sub>Cl (Calbiochem). The ECL-Plus kit was obtained from Amersham-Pharmacia Biotech. The  $\beta$ -amyloid 1–40 and 1–42 Colorimetric ELISA kit was purchased from Biosource International Inc.

### ***cDNA Constructs***

Expression vectors for all four human Numb isoforms have been described previously<sup>26</sup>,<sup>27</sup>. Full-length Numb, PTB deletion mutants of human Numb, or control expression plasmids were constructed as in-frame fusions downstream of the FLAG epitope. The plasmid for the dominant negative dynamin (dyn 1K44E tagged to HA and EGFP) was a kind gift from Dr. N. Bunnett, University of California at San Francisco. The cDNA encoding dyn 1K44E was subcloned into the retroviral vector pBabe-puro (Addgene). The construct was transfected together with a plasmid encoding the vesicular stomatitis virus membrane glycoprotein (VSV-G) envelope into 293T packaging cells (Clontech) using FuGENE-6, and the resulting virus-containing supernatant was collected at 48 and 72 h after transfection, and used for transduction as described<sup>28</sup>. Expression of exogenous dyn 1K44E was confirmed by immunoblotting.

### ***Cell lines and transfections***

PC12, HEK293 and SH-SY5Y cells were cultured under standard conditions in DMEM containing 10% fetal bovine serum (Invitrogen) and maintained at 37 °C in a 5% CO<sub>2</sub>/95% air atmosphere. The PC12 cells stably expressing Numb variants have been described previously<sup>27</sup>. SY5Y neuroblastoma cells stably transfected with a construct carrying the AD disease-linked double (“Swedish”) mutation K595N/M596L in APP were obtained from Dr. W. Araki (National Institute of Neuroscience, Tokyo, Japan).

## ***Treatments***

Trophic factor withdrawal was accomplished by washing the cells twice with phosphate-buffered saline (PBS) and then maintaining them in Locke's buffer<sup>26</sup>. DAPT (2 $\mu$ M) was used to inhibit  $\gamma$ -secretase activity. To inhibit proteasomes and lysosomes, cells were treated with proteasomal inhibitors MG-132 (5  $\mu$ mol/L) and *clasto*-lactacystin  $\beta$ -lactone (5  $\mu$ mol/L), or the lysosomal inhibitors chloroquine (100  $\mu$ mol/L) and NH<sub>4</sub>Cl (50 mmol/L) for various time periods. Inhibitors were resuspended either in dimethylsulfoxide (DMSO) or PBS. Controls were either treated with equivalent volumes of DMSO for the proteasome inhibitors or with equivalent volumes of PBS for chloroquine stimulations.

## ***RNA isolation and PCR***

Total RNA from cells grown on 100 mm dishes was isolated with Trizol (Invitrogen) and 2 $\mu$ g of RNA was reverse transcribed with Superscript II reverse transcriptase and an oligo-dT primer. Quantitative real-time PCR (RT-PCR) analyses of APP, Numb and actin were performed using the following pairs of primers: rat APP: 5'-CCACTACCACAACCTACCACTG-3' (forward) and 5'-CCTCTCTTTGGCTTTCTGGAA-3' (reverse); rat  $\beta$ -actin: 5'-TGTGATGGACTCCGGTGACGG-3' (forward) and 5'-ACAGCTTCTCTTTGATGTCACGC-3' (reverse); Rab5A: 5'-AACAAGACCCAACGGGCCAAATAC-3' (forward) and 5'-ATACACAACCTATGGCGGCTTGTGC-3'; PTB-Numb (forward): 5'-GGAAGTTCTTCAAAGGCTTCTTTG-3'; PTB-Numb (reverse): 5'-TTCATCCACAACCTCTGAGTCCATC-3'. The

Numb primers were designed to flank the alternatively spliced insert in the PTB domain of the rat Numb cDNA sequence (Accession No: NM\_133287).

### ***SDS-PAGE and Western blotting***

Cells were harvested and lysed in buffer (100 mM Tris, pH 6.8, 1% SDS, 10 mM EDTA, 5 mM EGTA, 2 mM PMSF, 25 µg/ml leupeptin, 5 µg/ml pepstatin). The lysates were cleared by centrifugation at 13,000 g for 20 min at 4°C. The protein content of cell lysates was measured using the bicinchoninic acid (BCA) reagent (Pierce). Extracts containing 50 µg of protein were electrophoresed using Tris-HCl or 16.5 % Tris-Tricine SDS-PAGE (BioRad) under reducing conditions and immunoblotted onto nitrocellulose membranes (Bio-Rad). For immunodetection of blots, enhanced chemiluminescence (ECL, Amersham) was applied. The optical band densities were quantified using NIH Image Analysis software.

### ***Immunofluorescence microscopy***

Following experimental treatments, cells were fixed for 20 min in 4% paraformaldehyde in PBS at room temperature, permeabilized (or not) with 0.2% Triton X-100 in PBS, incubated for 1 h in blocking solution (0.2 % Triton X-100, 5 % normal horse or goat serum in PBS) and then with primary antibody for 1 h in blocking solution at room temperature. The cells were washed with PBS and finally incubated with 1 µg / ml Alexa Fluor 488 goat anti-rabbit IgG (1 µg / ml, Molecular Probes) in blocking solution at room temperature for 1 h. When double labeling was required, cell preparations were incubated with Alexa Fluor 488-conjugated anti-mouse IgG and rabbit Alexa Fluor 594-conjugated anti-goat IgG (1:200). Immunostained cells

were observed with the appropriate filters on a Leica confocal laser scanning microscope; average pixel intensity per cell was determined using software supplied by the manufacturer. Appropriate controls, such as secondary antibody alone, indicated a lack of non-specific staining.

### ***Measurements of sAPP levels***

For detection of sAPP, the media were collected from cultures of PC12 clones and centrifuged at 3,500g (10 min, 4 °C) to remove cell debris. The cleared supernatants were concentrated at least 20 fold by ultrafiltration. Cells were harvested, lysed, and prepared for protein determinations. Equal amounts of volumes of supernatants, standardized to lysates protein, were subjected to SDS-PAGE and immunoblotting analyses. All conditioned media values were normalized to total protein lysates.

### ***A $\beta$ 40/42 sandwich enzyme-linked immuno-sorbent assay (ELISA) assay***

SH-SY5Y cells expressing the Swedish mutant APP were transfected with plasmids for the Numb variants or an empty pcDNA3 vector using Lipofectamine reagent according to the manufacturer's specifications. Conditioned media from transfected cells were collected 48 h after transfection, and protein inhibitors and AEBSF (Sigma) were added to prevent the degradation of A $\beta$ . The concentration of A $\beta$ 40/42 in samples and standards was measured in duplicates using the  $\beta$ -amyloid 1–40 and 1–42 colorimetric ELISA kit according to the manufacturer's instructions (Biosource).

### ***Measurements of secretase activity***

The activity of APP secretases was determined using commercially available secretase kits (R&D Systems) according to the manufacturer's protocol. The method is based on the secretase-dependent cleavage of a secretase-specific peptide conjugated to the fluorescent reporter molecules EDANS and DABCYL, which results in the release of a fluorescent signal that can be detected using a fluorescence microplate reader (excitation at 355 nm /emission at 510 nm). The level of secretase enzymatic activity is proportional to the fluorimetric reaction.

### ***Cell surface biotinylation***

Confluent 10 cm dishes of each of the PC12 clones were washed three times with ice-cold PBS supplemented with 1 mM Ca<sup>2+</sup> and 2 mM Mg<sup>2+</sup>, and incubated with 1 ml of biotin label (Pierce EZ-Link Sulfo-NHS-Biotin) at 2 mg/ml for 0.5 h on ice in the dark on a rotary mixer. The reaction was stopped by extensive washing with PBS and quenched with 50 mM glycine in PBS. Cell lysates were then immunoprecipitated with streptavidin-coated agarose. The precipitated biotinylated proteins were subjected to immunoblotting to analyze the content of APP and transferrin receptor.



## ***Results***

### ***Expression of Numb proteins alters APP metabolism in a manner dependent upon the PTB domain.***

To investigate the impact of Numb on APP metabolism, we stably overexpressed each of the four human Numb proteins in PC12 cells<sup>26, 27</sup>. APP is physiologically processed by  $\alpha$ -secretase or  $\beta$ -secretase resulting in the shedding of nearly the entire ectodomain to yield large soluble APP derivatives (called sAPP $\alpha$  and sAPP $\beta$ , respectively) and generation of membrane-tethered carboxyl-terminal fragments of APP (APP-CTFs) that include C83 and C99. The C99 is further cleaved by  $\gamma$ -secretase to release the ~4 kDa A $\beta$  peptide and the APP intracellular domain (AICD). Stable expression of the SPTB-Numb proteins resulted in a significant accumulation of intracellular APP (**Fig. 4A**) and increased secretion of sAPP $\alpha$  and sAPP $\beta$  in the conditioned media (**Fig. 4B**). By densitometric scanning of Western blots, the total amount of APP holoprotein in cells overexpressing the SPTB-Numb proteins was increased by four to five fold compared to parental control cells and by eight to ten fold compared to the LPTB-Numb clones. The increased accumulation of APP was confirmed by immunostaining using antibodies to the amino- and carboxyl-termini of APP (**Fig. 4B**).

The intracellular accumulation of APP holoprotein coincided with a significant increase in the amount of APP processing products. Both total sAPP and the amount of sAPP $\alpha$  immunoprecipitated from the conditioned media with anti-APP antibodies 22C11 and 6E10, respectively, were significantly higher in the SPTB-Numb clones. Steady-state levels of the  $\alpha$ -secretase- and  $\beta$ -secretase derived APP-CTFs, C83 and C99, respectively, were also increased in lysates, consistent with the ability of the SPTB-Numb proteins to promote non-amyloidogenic and amyloidogenic processing pathways (**Fig. 4B**). The opposite effect was observed in the

clones expressing LPTB-Numb; steady state levels of APP holoprotein and APP processing products were markedly reduced relative to the parental clones. Only with long exposure times could the sAPP and APP-CTFs in the LPTB-Numb clones be detected. In contrast to APP, no change in the total levels of the transferrin receptor (TfR; **Fig. 4A**) was found in the lysates suggesting that the observed effects mediated by the Numb proteins were selective for APP. Collectively, the data indicate that the Numb proteins that differ in the PTB domain affect the processing of APP in a distinct and contrasting manner.

***Expression of Numb proteins alters A $\beta$  generation in a manner dependent upon the PTB domain.***

Since the Numb proteins differentially affect APP cleavage and the generation of APP-CTFs, we reasoned that Numb should also influence the generation of A $\beta$ . To test this notion, the cDNAs encoding Flag-Numb variants were transfected into SY5Y cells expressing the Swedish mutant APP (**Fig. 4C**). A $\beta$ 40 and A $\beta$ 42 levels in the conditioned medium 48 h after transfection were determined using ELISA measurements. Consistent with the observed effects of Numb on the generation of APP-CTFs, we found that the LPTB-Numb proteins suppressed the production of A $\beta$ 40 and A $\beta$ 42 into the conditioned medium, whereas cells expressing the SPTB-Numb proteins generated elevated levels of A $\beta$ 40 (7.3 pg/ml versus 28.5 pg/ml/protein) and A $\beta$ 42 (3.4 pg/ml/protein versus 13.2 pg/ml) normalized to the total protein amount (**Fig 4C**).

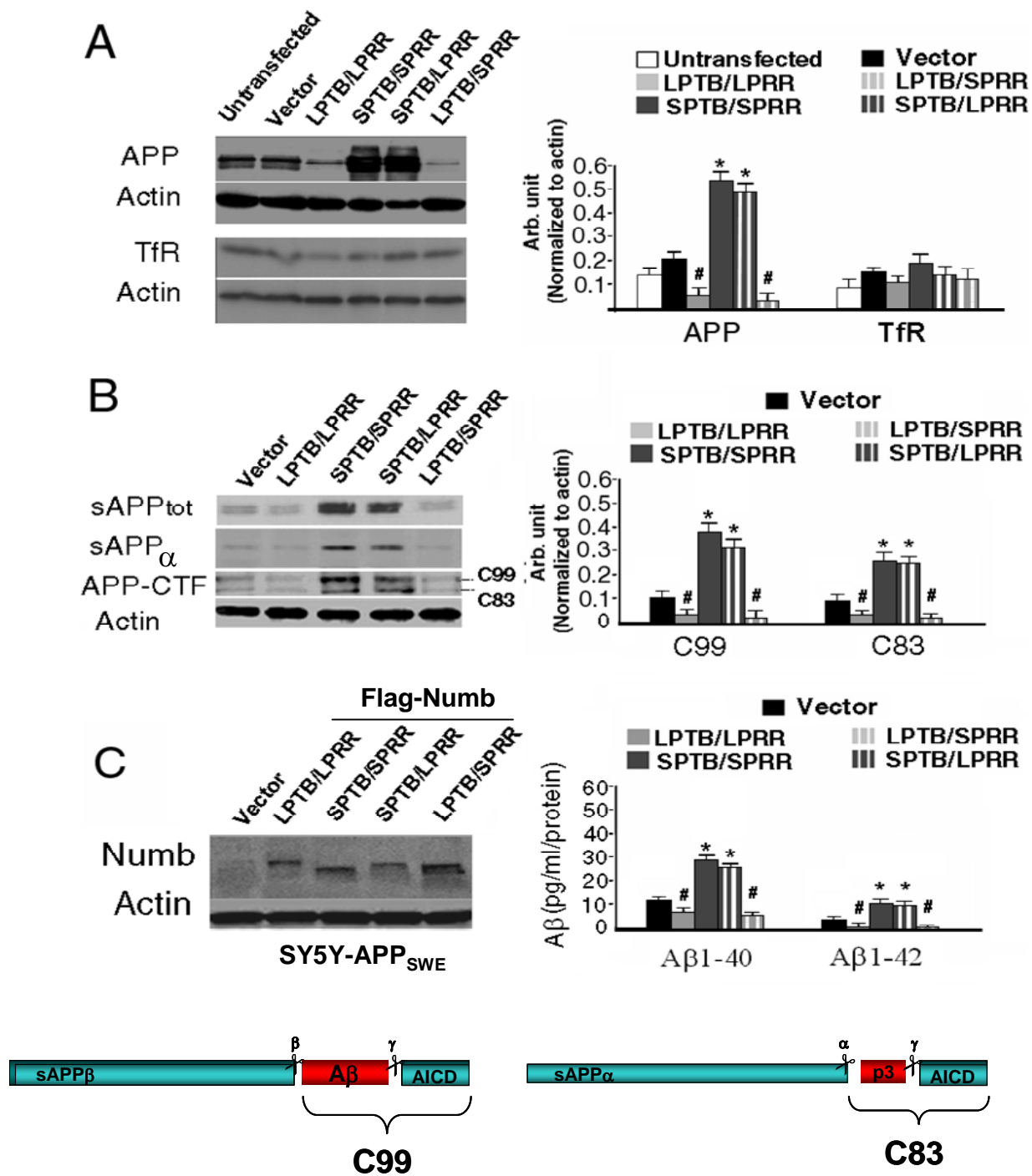


**Figure 4.** Isoform specificity in the processing of APP and generation of A $\beta$  by the Numb proteins.

(A) Effect of Numb proteins on the amounts of APP and TfR. Representative immunoblot showing total levels of APP and TfR protein in the indicated PC12 clones (left panels). Each lane was loaded with 50  $\mu$ g of protein. The relative amounts of APP and TfR were normalized to those of actin. Densitometric analyses were performed on the immunoblots (right panel). The values in the histogram represent the mean  $\pm$  SD  $n = 3$ ; \* $p < 0.01$ ; # $p < 0.05$  (ANOVA with Scheffe post-hoc tests) relative to empty vector-transfected cells. (B) Effect of Numb proteins on the cleavage of APP. APP derivatives in the conditioned medium and in lysates of the indicated PC12 clones were quantified by western blot followed by densitometric analyses. APP derivatives in conditioned culture medium were immunoprecipitated with an antibody to the amino terminal domain of the APP protein (22C11 which precipitates both sAPP $\alpha$  and sAPP $\beta$  and an antibody to A $\beta$  (6E10; Signet) which recognizes sAPP $\alpha$ . Steady-state levels of membrane-associated APP derivatives, C99 and C83, were immunodetected with antibodies to the carboxyl terminal domain of the APP protein. The  $\beta$ -actin signal represents the internal loading control. Densitometric analyses were performed on the immunoblots (left panel). The values in the histogram represent the mean  $\pm$  SD;  $n = 3$ ; \*  $p < 0.01$ ; #  $p < 0.05$  (ANOVA with Scheffe post-hoc tests) relative to vector-transfected control. Essentially similar results were obtained using two additional stable clones. (C) Effect of Numb proteins on the generation of A $\beta$  peptides. SY5Y cells stably expressing the Swedish mutation of APP were transfected with plasmids encoding the Flag-Numb proteins. Conditioned media were harvested and analyzed by a sandwich-ELISA for specific quantization of A $\beta$ 40 and A $\beta$ 42. Expression of Flag-Numb proteins was detected by immunoblotting using an antibody to Flag (left panels). The histogram shows the amounts of A $\beta$ 40 and A $\beta$ 42 in the indicated clones (right panels). The values represent the mean  $\pm$  SD;  $n = 3$ ; \* $p < 0.01$ ; # $p < 0.05$  (ANOVA with Scheffe post-hoc tests) relative to vector-transfected cells.

***Expression of the Numb proteins does not affect the level of APP expression nor the proteolytic activities of the APP processing secretases.***

One possible explanation for the effects of Numb on APP metabolism would be an alteration in the expression of APP. The presence of the Numb proteins had no significant effect on the levels of APP mRNA (**Fig. 5A**). We also considered the possibility that the Numb proteins might differentially alter the activities or the amounts of the APP processing secretases. To investigate the influence of the Numb proteins on APP cleavages, we analyzed the proteolytic activities of  $\alpha$ -,  $\beta$ -, and  $\gamma$ -secretases using commercially available secretase kits from R&D Systems. No significant difference in the proteolytic activities of these secretases was detected among the stable clones (**Fig. 5B**). In addition, we found that levels of BACE1 and of the  $\gamma$ -secretase components (presenilin-1, nicastrin, APH-1, APH2) were not altered by the expression of Numb (**Fig. 5C**) which further argued against a role of the Numb proteins in regulating the proteolytic activities of the secretases. Collectively, the data suggest that Numb proteins do not alter APP metabolism by regulating the expression of APP or the enzymatic activities of the secretases.

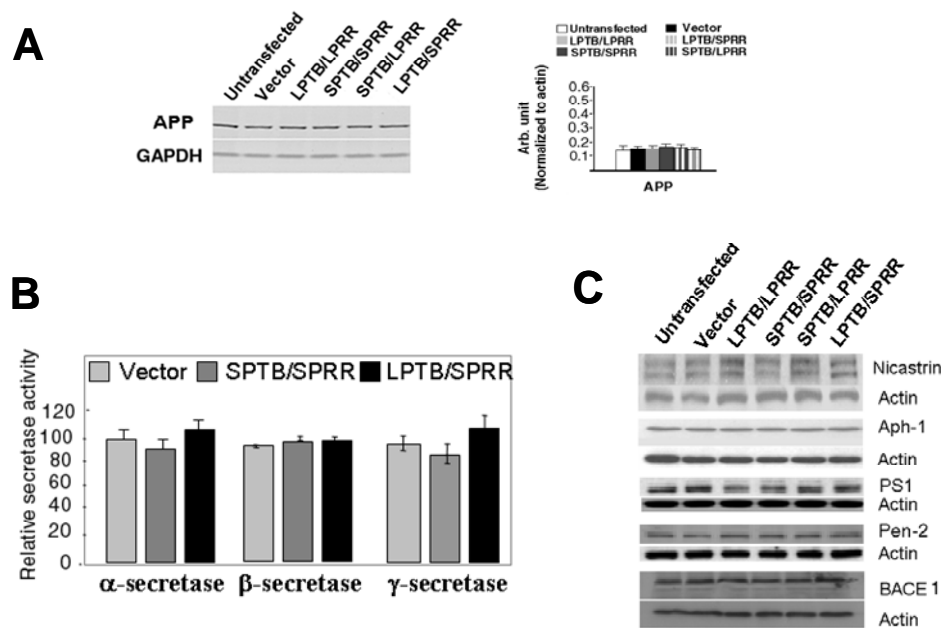


**Figure 5. Lack of isoform specificity on the expression of APP and the activities of the APP secretases**

(A) Expression of the Numb proteins did not alter the expression of APP. Semi-quantitative RT-PCR analysis of APP mRNA in the indicated PC12 clones (left panels). The GAPDH signal represents the internal loading control. The values in the histogram are the mean  $\pm$  SD of 3 independent measurements (right panel). Essentially similar results were obtained using two additional stably transfected clones. (B) Expression of the Numb proteins did not alter the activities of APP processing secretases. The lysates were tested for secretase activities by addition of secretase specific peptide substrates conjugated to the reporter molecules EDANS and DABCYL (R&D). Fluorescently labeled peptides were detected only upon cleavage by the respective secretases. After incubation at 37  $^{\circ}$ C for 2 h, reactions were transferred to a 96-well plate, and fluorescence was measured as described under "Experimental Procedures". The values expressed as arbitrary units of fluorescence (AUF), are the mean  $\pm$  SD of at least 3 independent experiments. (C) Numb proteins did not alter the protein level of  $\beta$ -secretase (BACE1) and of the components of the  $\gamma$ -secretase complex. Representative immunoblots showing total levels of  $\beta$ -secretase, presenilin-1, nicastrin, Aph-1, and Pen-2 in the indicated clones. Each lane was loaded with 50  $\mu$ g of protein. Blots were reprobed with an antibody against actin to confirm equal levels of protein loading among samples.

### ***The effects of Numb on APP metabolism is dependent on its interaction with APP and the internalization of APP***

Because the interaction of APP with Numb requires the YENPTY motif interacting with the PTB domain <sup>24</sup>, we determined the effects of a Numb deletion mutant lacking the PTB domain ( $\Delta$ PTB-Numb) on APP metabolism. Quantification of the Western blots (normalized to actin) revealed that APP metabolism was not altered in the presence of the  $\Delta$ PTB-Numb protein (**Fig. 6A**) suggesting that the PTB domain is required for the Numb proteins to influence APP metabolism. To determine if the Numb proteins affect the proteolytic processing of APP by targeting APP along the endocytic rather than the secretory routes, we examined the effects of a dominant negative mutant dynamin (dyn 1K44E tagged to the hemagglutinin epitope (HA) and EGFP; a gift from N. Bunnett, U of California at San Francisco) on the ability of each Numb protein to modulate APP metabolism. The GTPase dynamin is an important mediator of clathrin dependent endocytosis and is required for the internalization of many cell surface receptors including Notch and APP <sup>7, 29</sup>. As expected, inhibition of endocytosis by mutant dynamin induced an elevation of APP holoprotein in all the clones including the LPTB-Numb clones (**Fig. 6B**). Total APP protein level in the SPTB-Numb and LPTB-Numb clones was not significantly different compared to those in the vector-transfected and parental clones. These results indicate that the Numb proteins differentially affect the processing of APP along the endocytic route.

### ***Numb proteins influence the endosomal trafficking of APP***

APP undergoes a retrograde transport back to the cell body wherein it is localized in Rab5a positive early endosomes <sup>30</sup>, late endosomes <sup>8,31</sup>, lysosomes <sup>6</sup> and the Golgi-complex <sup>8</sup>. To

determine whether the Numb proteins affect the transport of APP to these intracellular compartments, we applied immunofluorescence microscopy to examine the subcellular localization of APP and Numb. Both these proteins are colocalized on the plasma membrane and in vesicular structures in PC12 cells (**Fig. 6C**). Expression of the SPTB-Numb proteins resulted in a marked accumulation of APP in enlarged endosomes (**Fig. 6D**) that were positively labeled for Rab5a (**Fig. 6E**). Increased APP immunoreactivity was also detected in Rab11-labeled recycling endosomes (data not shown) but not in LAMP1-labeled lysosomal compartments of the SPTB-Numb clones (data not shown). The subcellular location of APP was similar to that of Numb suggesting that Numb interact with APP in the early endocytic compartments. By contrast, APP was only faintly detected in the Rab5- (**Fig. 6D**), Rab11-, and LAMP1-labeled compartments (data not shown) in LPTB-Numb clones. Collectively, these data suggest that the PTB domain of Numb determines the processing fates of APP by regulating its endosomal sorting and trafficking to distinct compartments.



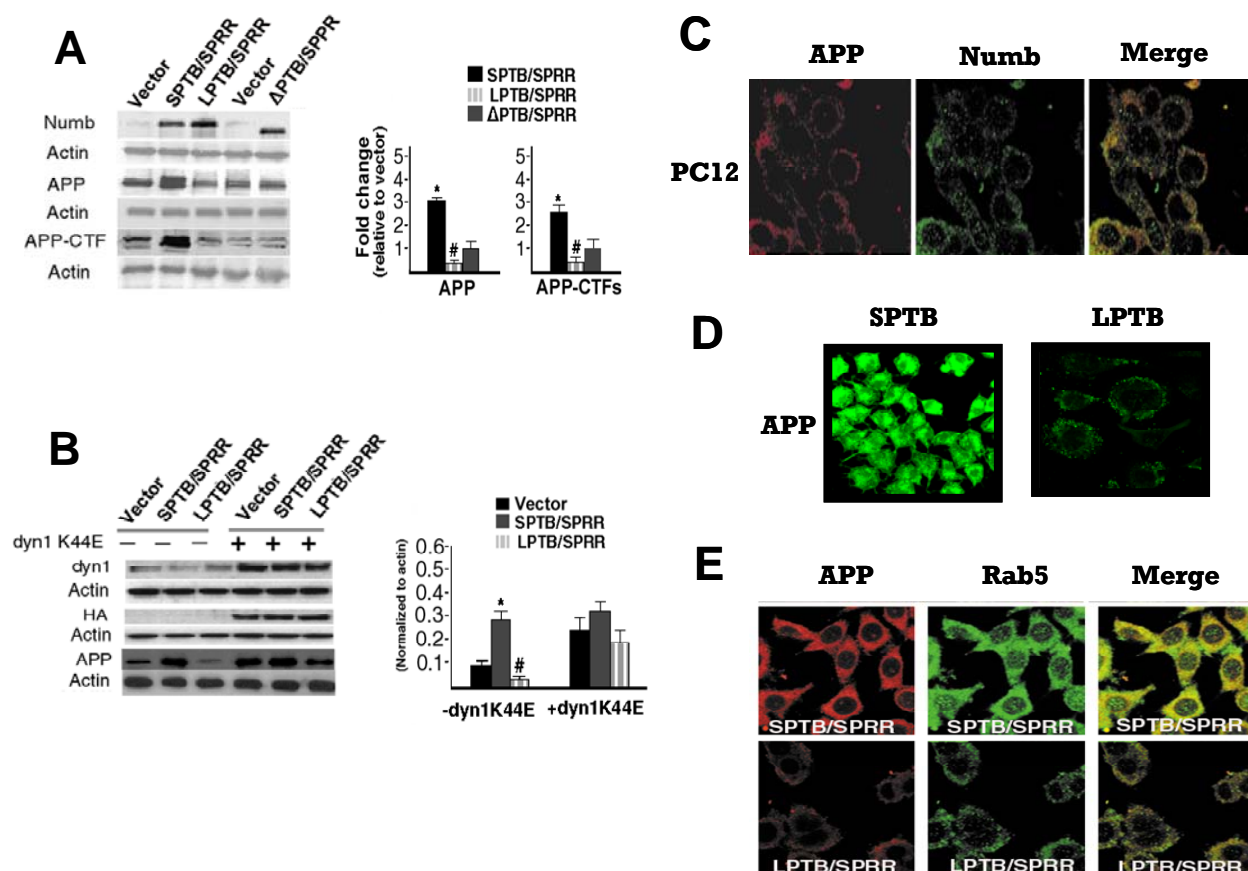


**Figure 6. Isoform specificity of Numb effects on APP metabolism is dependent on the interaction of the Numb proteins with APP and its subsequent internalization**

**(A)** Expression of a Numb protein lacking the PTB domain ( $\Delta$ PTB-Numb) did not alter APP metabolism. Representative immunoblot showing total levels of APP holoprotein in the indicated PC12 clones (left panels). Each lane was loaded with 50  $\mu$ g of protein. APP was quantified by western blot with an antibody to the amino terminal domain of the APP protein followed by densitometric analyses (right panel). The relative amounts of APP were normalized to those of actin. **(B)** Inhibition of endocytosis by overexpression of mutant dynamin (dyn) 1K44E abolished the effects of the Numb proteins on APP metabolism. Twenty-four hours after transduction, cell lysates were analyzed by immunoblotting followed by densitometry (right panel). Representative Immunoblot showing total levels of APP in the indicated PC12 clones. Overexpression of the dyn1K44E was confirmed using antibodies raised to dyn1 and to the HA tag. The  $\beta$ -actin signal represents the internal loading control. The values in the histogram represent the mean  $\pm$  SD n = 3; \*p < 0.01; #p < 0.05 (ANOVA with Scheffe post-hoc tests) relative to vector-transfected cells. **(C)** Localization of APP and Numb in PC12 cells by confocal immunofluorescence microscopy. Following fixation and permeabilization, rabbit anti-Numb and goat anti-rabbit conjugated FITC, and mouse anti-APP (22C11) and goat anti-mouse conjugated CY3 secondary antibody were used to detect Numb and APP protein, respectively. The right panel shows the merged image of APP and Numb. **(D)** Intracellular accumulation of APP and membrane-associated APP derivatives in a SPTB-Numb (left panel) and LPTB-Numb clone (right panel). Following fixation and permeabilization, APP was detected with antibodies to the carboxyl terminal domains of the APP protein. **(E)** Localization of APP to endocytic compartments by confocal immunofluorescence microscopy. Following fixation and permeabilization, rabbit anti-Rab5A and goat anti-rabbit conjugated FITC were used to detect the early endosomes (green signal), and mouse anti-APP (22C11) and goat anti-mouse conjugated CY3 secondary antibody were used to detect APP protein (red signal). The right side of each image shows the merged image of APP and Rab5, depicting early endosomes. The images are representative of those obtained from at least three stably transfected clones.

### ***Effect of the Numb proteins on the endosomal sorting of APP to the recycling pathway***

In spite of the accumulation of APP in the enlarged early endosomes (**Fig. 6D**), SPTB-Numb clones exhibited increased release of sAPP $\alpha$  and generation of C83 suggesting that APP may be preferentially sorted from the early endosomes back to the cell surface where APP is cleaved by  $\alpha$ -secretase. To evaluate the amount of APP localized on the cell surface, we performed cell membrane staining for APP on ice without permeabilization. Only a small fraction of APP was detected at the cell surface of parental cells not permeabilized prior to antibody incubation (**Fig. 7A**), consistent with a previous report <sup>5</sup>. The fraction of cell surface-bound APP was markedly higher in the SPTB-Numb clones. As expected, this fraction was significantly lower in the LPTB-Numb clones compared to parental cells. As another measure of surface APP protein level, proteins on the cell surface were biotinylated with a cell impermeable cross-linker, collected with streptavidin-coupled beads, and subjected to immunoblotting. As expected, the level of biotinylated plasma membrane-bound APP was significantly higher in SPTB-Numb clones (**Fig. 7B**). By densitometric scanning of Western blots, the amount of cell surface-localized APP relative to TfR was approximately five folds higher in cells overexpressing SPTB-Numb compared to vector-transfected cells (**Fig. 7C**). None of the biotinylated fractions contained actin consistent with the labeling of only cell surface bound proteins (**Fig. 7B**).

To determine whether vesicle recycling contributed to the increased cell surface expression of APP in the SPTB-Numb clone, we assessed the impact of a blockade in the endosome recycling pathway. Preincubation with monensin, an established inhibitor of the recycling pathway that does not interfere with the initial endocytosis of surface receptor proteins

<sup>32</sup>, significantly depleted cell surface APP expression as assessed by surface biotinylation followed by immunoblotting of the isolated biotinylated fraction (**Fig. 7D**). The surface receptor depleting effect of monensin on TfR was only slightly reduced in the absence of ligand (**Fig. 7D**) suggesting that the recycling pathway of APP may be mechanistically distinct from that of TfR. Quantification of the immunoblots revealed that the changes in the ratio of APP to TfR after treatment with monensin was significantly greater in the SPTB-Numb clone compared to the vector-transfected cells (**Fig. 7E**).

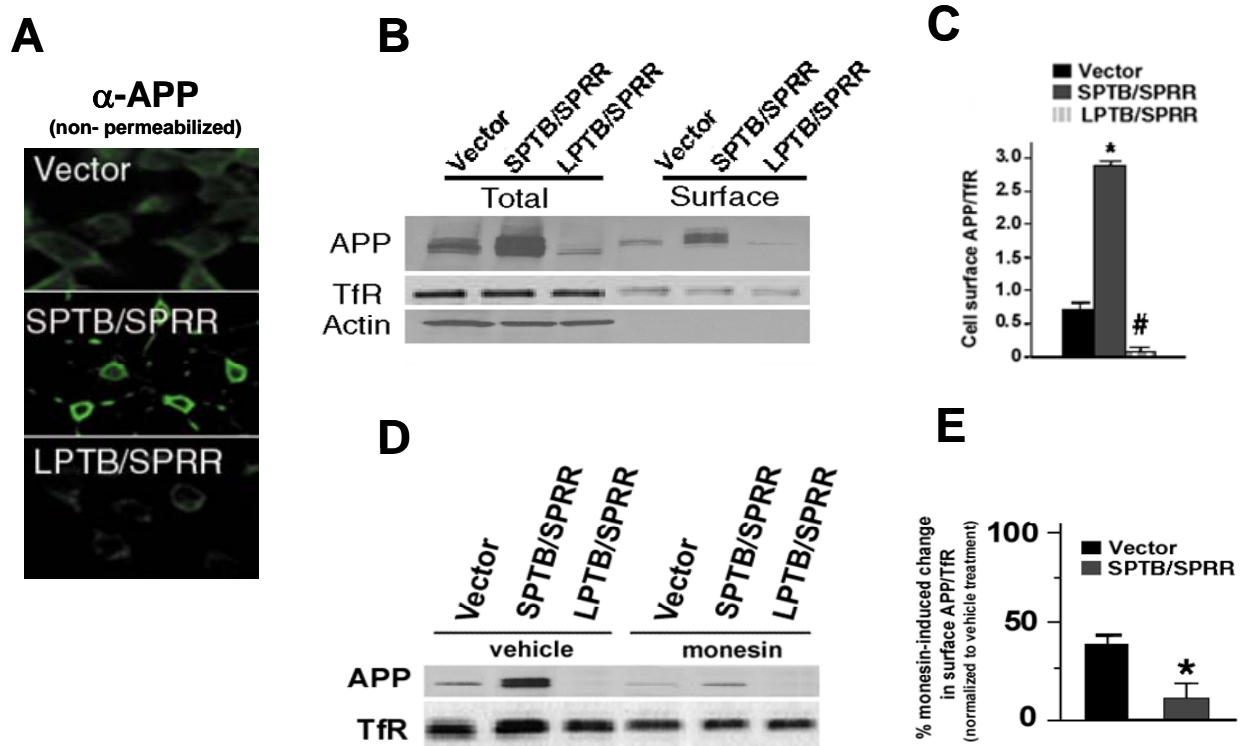


**Figure 7. Effect of the Numb proteins on the sorting of APP to the recycling pathway**

(A) The Numb proteins differentially alter the amount of cell surface APP. Immunostaining of cell surface APP with an antibody to the amino terminal end of APP. In non-permeabilized cells (without Triton X-100), significantly more APP is detected on the surface of a SPTB-Numb clone compared to a LPTB-Numb clone or a clone transfected with empty vector. (B) Detection of cell surface APP by biotinylation. Cells were surface biotinylated, lysed, and incubated with streptavidin-agarose beads. Biotinylated proteins were immunoblotted with antibodies to APP and TfR. (C) Quantitative data showing the ratio of cell surface APP and TfR in the indicated clones. Values are the mean  $\pm$  SD of at least 3 independent experiments. \* $p < 0.01$ ; # $p < 0.05$  (ANOVA with Scheffé post-hoc tests) relative to vector-transfected cells. (D) Recycling blockade depletes cell surface APP protein level. The indicated clones were pretreated with monensin for 60 min at 37°C in DMEM/BSA and incubated in DMEM/BSA for 60 min afterwards. Cells were then surface biotinylated using a membrane-impermeable cross-linker and immunoprecipitated with streptavidin beads. Precipitates were subjected to SDS-PAGE, and blots were probed with antibodies to APP and TfR. (E) Quantitative data showing the changes in the ratio of cell surface APP and TfR in the vector-transfected and a SPTB-Numb clone after monensin treatment. Values are plotted as percent of untreated control (vehicle) and are the mean  $\pm$  SD of at least 3 independent experiments. \*  $p < 0.05$  (Student's t test) relative to vector-transfected cells.

### ***Effects of the Numb proteins on the endosomal sorting of APP to the degradative pathway***

To further establish that altered subcellular localization of APP is responsible for the differences in its processing fates in the Numb clones, we treated PC12 clones with chloroquine, a weak base known to disrupt lysosomal function by blocking organelle acidification<sup>33</sup>. Treatment with chloroquine (100  $\mu$ M) for up to 6 h (**Fig. 8A**) and longer (data not shown) had no marked effects on the levels of APP (**Fig. 8A**) and APP-CTF derivatives (data not shown) in SPTB-Numb clones. Similar results were obtained in the presence of ammonium chloride

(NH<sub>4</sub>Cl; 50 mmol/L) confirming that the available pools of APP in the SPTB-Numb cells were absent from the lysosomes (**Fig. 8B**). By contrast, levels of APP protein (**Fig. 8A**) and APP-CTF derivatives (data not shown) in LPTB-Numb clones were significantly increased following chloroquine treatment in comparison to vector-transfected cells, ruling out the possibility that chloroquine at the concentration of 100 μM was too low to induce APP accumulation in the SPTB-Numb clone (**Fig. 8A**). The same dose of chloroquine also caused marked accumulation of APP and APP-CTFs in SH-SY5Y cells stably transfected with the empty vector or with the Swedish mutant APP (**Fig. 8C**). The effect of lysosomal inhibitors on APP protein levels was dose-dependent (data not shown). Control incubation of PC12 clones with PBS resulted in unchanged levels of APP (data not shown). To determine that the chloroquine-induced increase in APP holoprotein was not related to an effect of Numb on the synthesis of APP, we treated cells with the protein synthesis blocker cycloheximide (10 μg/mL) in combination with chloroquine. Treatment with cycloheximide for 6 h did not prevent the chloroquine-induced increase in APP holoprotein (data not shown).

In contrast to lysosomal inhibitors, we found that treatment with the γ-secretase inhibitor DAPT markedly enhanced steady state levels of APP and APP-CTFs in the SPTB-Numb clone (**Fig. 8D**). The APP-CTFs were only weakly detected in the vector cells but became clearly visible, as in the untreated SPTB-Numb clones, after treatment with DAPT which halted the cleavage of membrane associated APP-CTFs. The effect of DAPT on APP protein levels was dose-dependent (data not shown). In contrast, DAPT failed to elevate levels of APP-CTFs in the LPTB-Numb clones. Collectively, our data indicate that the Numb proteins target APP to endocytic compartments with distinct APP processing outcomes.

***The proteasome-mediated degradative pathway is not involved in the regulation of APP metabolism by the Numb proteins***

Considerable evidence indicates that Numb antagonizes Notch signaling transduction by activating the endocytic uptake and degradation of the Notch protein via the proteasomal degradation pathway<sup>19, 34</sup>. Because of the striking similarities in the proteolytic processing of Notch and APP, we hypothesized that the LPTB-Numb proteins may reduce APP protein levels by facilitating proteasomal-mediated degradation of APP. To test this hypothesis, we treated the stable clones with lactacystin, which inhibits proteasomal degradation of proteins by specifically targeting the 20S proteasome, without interfering with lysosomal protein degradation<sup>35</sup>. Treatment with lactacystin did not result in significant changes in APP protein levels and did not impact the generation of APP metabolites in any of the clones tested (**Fig. 8E**) suggesting that the differential effects of the Numb proteins on APP metabolism did not involve the ubiquitin-proteasome protein degradation pathway. Higher concentrations of lactacystin did not significantly induce APP accumulation although the dose of 10  $\mu$ M was sufficient to induce enrichment of ubiquitinated protein species in general, as shown in Western blot analysis conducted with an antibody to ubiquitin (data not shown). Collectively, the data indicate that the drastic reduction in APP protein level in the LPTB-Numb clones was not due to Numb-mediated targeting of APP for proteasome-dependent degradation.

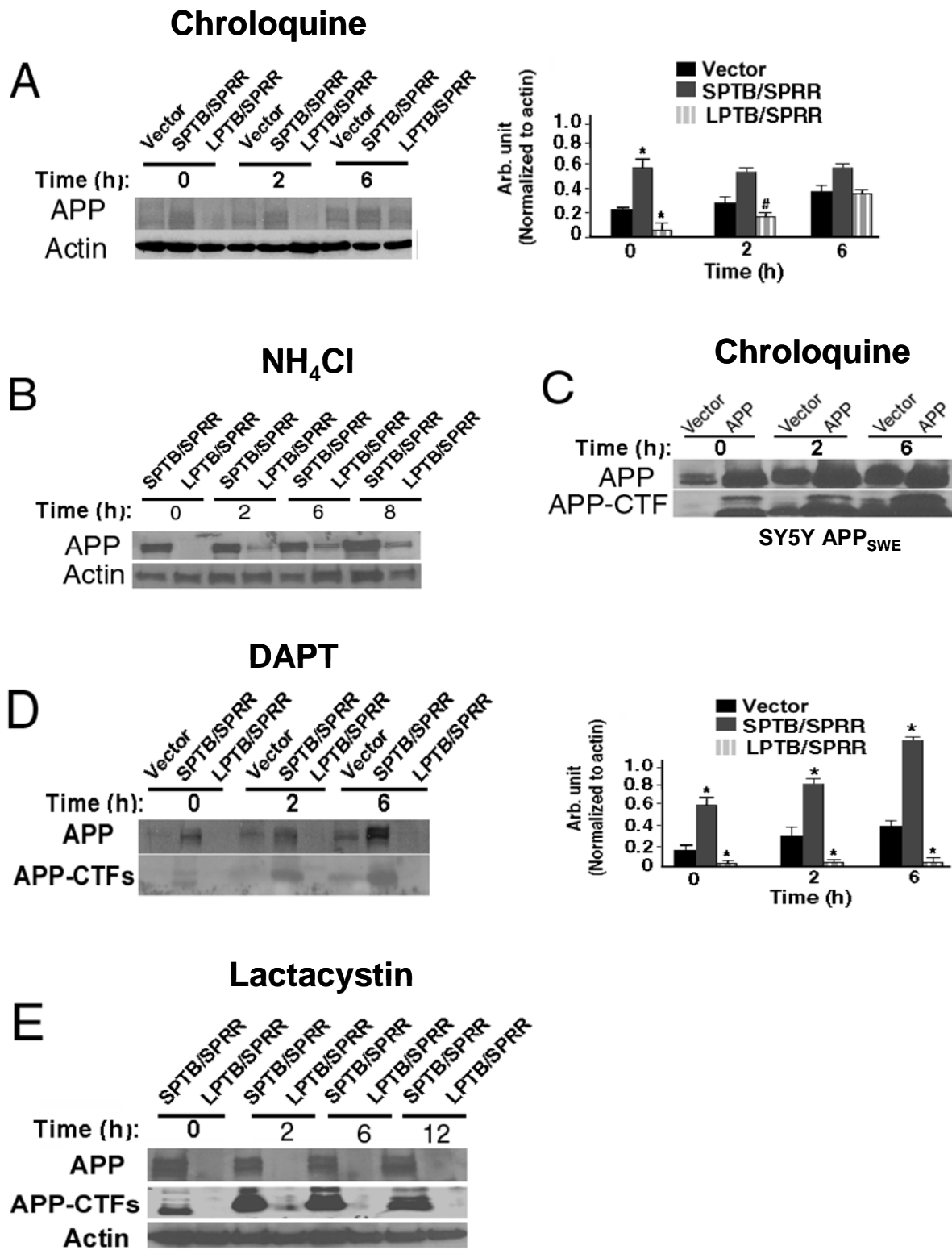


Figure 8. Effect of the Numb proteins on the sorting of APP to the degradative pathway



(A) Time course of the accumulation of APP and APP-CTFs in LPTB-Numb but not SPTB-Numb clones after treatment with a lysosomal inhibitor. The indicated stable PC12 clones were treated with chloroquine (100  $\mu$ M) for 0, 2, and 6 h. Equal amounts of cellular lysates were separated by 16.5% Tris-Tricine SDS-PAGE and immunoblotted with an antibody to the carboxyl terminal of APP.  $\beta$ -actin was used as the internal loading control. Densitometric analyses were performed on the immunoblots (bottom panel). The values in the histogram are the mean  $\pm$  SD of 3 independent measurements. \* $p$ < 0.01, # $p$ <0.05 (ANOVA with Scheffe post-hoc tests) relative to vector-transfected cells. Similar results were obtained using two additional stably transfected Numb clones. (B) Time course of the accumulation of APP in LPTB-Numb but not SPTB-Numb clones upon treatment with NH<sub>4</sub>Cl. The indicated clones were treated with NH<sub>4</sub>Cl (50  $\mu$ M) for 0, 2, 6, and 8 h and processed for immunoblotting using an antibody to the carboxyl terminal of APP. (C) Time course of the accumulation of APP and APP-CTFs in SH-SY5Y cells overexpressing the empty-vector (Vector) or a vector encoding the Swedish mutant APP (APP) upon chloroquine treatment. The indicated SY-SY5Y clones were treated with chloroquine (100  $\mu$ M) for 0, 2, and 6 h. Each lane was loaded with 50  $\mu$ g of protein.  $\beta$ -actin was used as the internal loading control. (D) Time course of the accumulation of APP in the SPTB-Numb but not LPTB-Numb clones after treatment with the  $\gamma$ -secretase inhibitor DAPT. The indicated clones were treated for 0, 2, 6, and 12 h with 10  $\mu$ M DAPT. Each lane was loaded with 50  $\mu$ g of protein.  $\beta$ -actin was used as the internal loading control. Densitometric analyses were performed on the immunoblots (bottom panel). Values are the means  $\pm$  SD of 3 independent measurements. \* $p$ < 0.01 (ANOVA with Scheffe post-hoc tests) relative to empty vector transfected cells. (E) Inhibition of the proteasomes failed to affect the regulation of APP metabolism by the Numb proteins. Time course of the levels of APP and APP-CTFs in the indicated clones after treatment with 10  $\mu$ M lactacystin. Equal amounts of protein from each sample were immunoblotted to detect APP and APP-CTFs. Each lane was loaded with 50  $\mu$ g of protein and verified with an antibody to actin. Essentially similar results were obtained using two additional stably transfected Numb clones.

### ***Expression of Numb proteins alters the levels of the Rab family of endocytic regulators***

Recent studies have demonstrated the involvement of GTP-binding proteins of the Rab family in the trafficking and processing of APP<sup>36, 37</sup>. Rab proteins are localized in both discrete organelles and vesicles where they play key roles in protein trafficking between compartments along the secretory and endocytic routes. To determine whether the differential endosomal sorting of APP resulted from the altered expression of Rab proteins, we measured protein levels of Rab4, Rab5A, Rab7, and Rab11. Rab5A is a small GTPase localized on early endosomes and controls endosome fusion along the endocytic pathway. Rab4A and Rab11 are regulators of the recycling endosomes<sup>36, 37</sup>. Protein levels of Rab4A, Rab5A and Rab11 were significantly increased in the SPTB-Numb clones relative to control cells (**Fig. 9A, B**). By contrast, levels of Rab5A and Rab11 were decreased in the LPTB-Numb clones relative to control cells (**Fig. 9A, B**). Levels of Rab7, a regulator of fusion events in the late endocytic pathway, and of LAMP-1, a lysosome-associated membrane protein-1 were not different among the stable clones (**Fig. 9A, B**). The changes in the level of the Rab5A protein were not attributable to altered expression as its mRNA level was not significantly different in the stably transfected Numb clones (**Fig. 9C**).

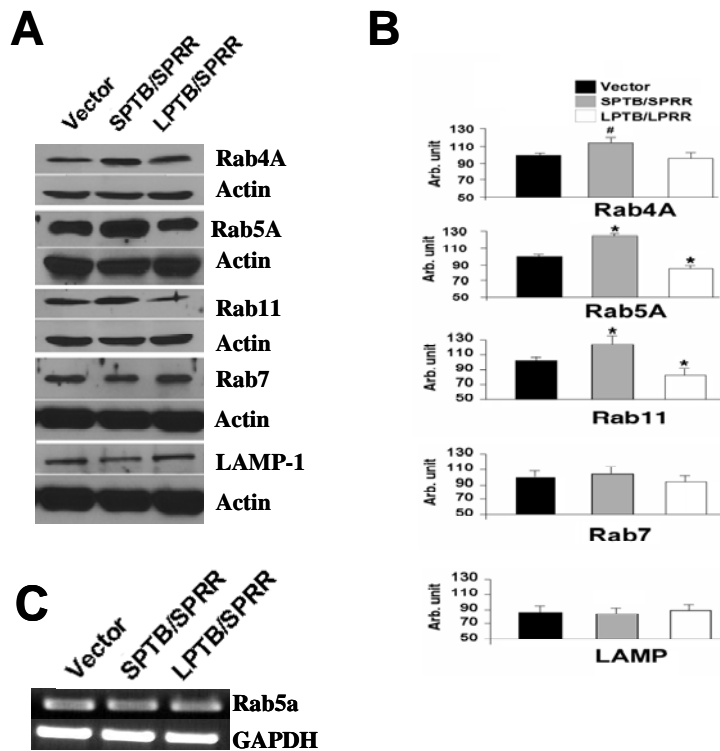


**Figure 9. Effect of the Numb proteins on the levels of small Rab GTPases**

(A) Representative Immunoblots showing total amounts of Rab4A, Rab5A, Rab7, Rab11, and LAMP1 in the indicated clones. Each lane was loaded with 50  $\mu$ g of protein and verified with an antibody to actin. (B) Densitometric analyses were performed on the immunoblots shown in (A). The values in the histogram are the mean  $\pm$  SD of 3 independent measurements. \* $p < 0.01$ , # $p < 0.05$  (ANOVA with Dunnett's Multiple Comparison Test). (C) Semi-quantitative RT-PCR analysis of Rab5A mRNA in the indicated PC12 clones. The GAPDH signal represents the internal loading control.

### ***Stress induces the selective upregulation of SPTB-Numb transcripts***

It has been previously reported that alternative splicing of Numb primary transcripts is developmentally regulated<sup>37, 38</sup>. To determine whether the balance of the alternative spliced variants of Numb might be disrupted in cells that were stimulated by apoptosis-inducing agents, we designed oligonucleotide primers that bind to the flanking sequences of the insertion in the

PTB domain (**Fig. 10A**). The expected sizes of the amplified PCR products for the SPTB- and LPTB-Numb transcripts were 114 and 147 base pairs, respectively. The level of LPTB-Numb mRNA which is predominantly expressed under basal condition decreased rapidly upon trophic factor withdrawal (TFW), an insult that has previously shown to alter Numb expression<sup>26</sup>, whereas that of SPTB-Numb accumulates in parallel in stressed cells (**Fig. 10B,C**). Protein but not mRNA levels of APP were also increased in PC12 cells subjected to TFW (data not shown). Collectively, these data suggest that cellular could induce the selective upregulation of SPTB-Numb proteins which precedes the accumulation of APP protein.

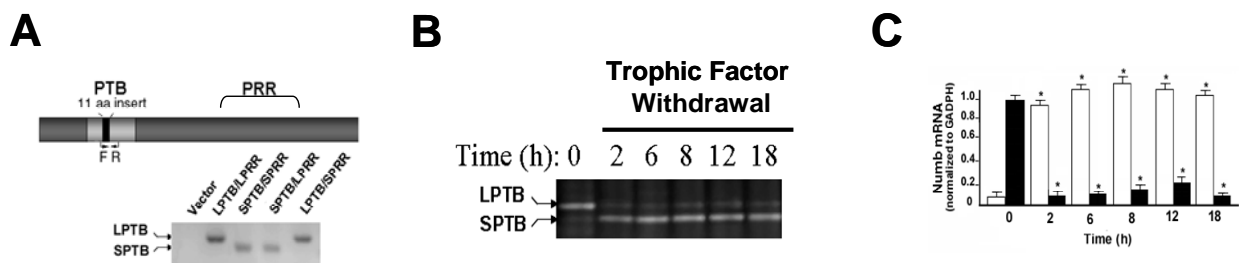


**Figure 10. Detection of alternatively spliced Numb transcripts under normal and stressed conditions**

(A) Domain structure of the Numb protein. The 11 amino acid insertion in the PTB domain is indicated in black. The forward (F) and reverse (R) primers were designed to amplify a region flanking the PTB insertion. The specificity of the primer set was confirmed by performing PCR using an empty plasmid (pCDNA3.1) or plasmids containing each of the four Numb isoforms. The expected sizes of PCR fragments were 114 and 147 base pairs for the SPTB- and LPTB-Numb transcripts, respectively. (B) Time course of SPTB-Numb and LPTB-Numb mRNA levels in PC12 cells subjected to trophic factor withdrawal. (C) Densitometric analyses were performed on the data shown in (B). The values in the histogram are the mean  $\pm$  SD of 3 independent measurements. \* $p < 0.01$  (Student's *t*-test) relative to untreated control PC12 cells.

## *Discussion*

Alterations in the endosomal-lysosomal system are believed to occur early in the disease process in AD, and may precede the formation of plaques and tangle-associated neuropathology in susceptible neuron populations. Endosome enlargement occurs early in sporadic AD, and is associated with increased endocytosis and endosome recycling. A $\beta$  immunoreactivity is evident in these populations of enlarged endosomes prior to A $\beta$  deposition indicating their potential importance for A $\beta$  formation in early AD brain. Much attention has focused on the mechanisms that regulate the trafficking of APP to endosomes. In this study, we have uncovered a novel function for the Numb adapter proteins as a regulator of endocytic trafficking of APP. Most surprisingly, we found that the Numb proteins that differ in the PTB, but not in the PRR domain, have opposite effects on the transport and processing of APP. The expression of SPTB-Numb proteins resulted in a significant accumulation and persistence of APP holoprotein in the early endosomes and increased A $\beta$  secretion. By contrast, expression of LPTB-Numb proteins significantly decreased the accumulation of APP and inhibits A $\beta$  secretion. The reduction in A $\beta$  secretion was not the result of either the decreased expression of APP or a significant reduction in the activities of the APP processing secretases. Furthermore, we demonstrated that all the Numb isoforms were capable of interacting with the APP holoprotein, as reported by a previous study<sup>24</sup>. The APP lowering effect was related to the trafficking role of the LPTB-Numb proteins along the endocytic rather than the secretory pathway as treatment with lysosomal inhibitors was able to restore endogenous APP holoprotein to the steady state level found in vector-transfected cells. It is conceivable that LPTB-Numb but not SPTB-Numb proteins facilitate the delivery of APP to the lysosomes for degradation by acidic hydrolases. Taken together, these results indicate that APP trafficking differs strikingly in the clones stably expressing the Numb proteins and raise

the intriguing possibility that alternative splicing of Numb could alter the trafficking of APP and, concomitantly, its processing fate.

Numb was discovered as an intracellular Notch antagonist<sup>15, 17</sup>. Considerable evidence over the past years indicated that Numb antagonizes Notch1 signaling by inducing Notch1 ubiquitination and endocytic degradation of NICD<sup>19, 35</sup>. Genetic and biochemical evidence in invertebrates has suggested that proteasomal degradation of Notch may be required for the cessation of Notch signaling<sup>19, 35</sup>. Numb has been shown to recruit the E3 ubiquitin ligase to facilitate Notch receptor ubiquitination<sup>19</sup>. Several E3 ubiquitin ligases such as LNX, Itch, Siah1, and Mdm2 have been shown to associate with Numb<sup>19, 39, 40</sup>. To exclude the possibility that the LPTB-Numb target APP for proteasomal degradation, we found that proteasomal inhibition had no marked effect on the accumulation of APP in the stable clones examined suggesting that Numb did not target APP for proteasomal degradation.

The PTB domain is a protein-protein interaction motif that has been identified in diverse group of proteins, of which only a subset is linked to tyrosine kinase-mediated signaling<sup>41</sup>. Structure-function analyses indicated that the Numb PTB domain can bind to multiple conformationally distinct peptide ligands in a phosphotyrosine-independent manner<sup>42-44</sup>. The PTB domain of Numb has been shown to interact with diverse proteins that determine its subcellular localization<sup>42</sup> and protein stability<sup>45</sup>. The PTB domain of Numb mediates the interaction with the E3 ubiquitin ligases responsible for the ubiquitination of its bound substrates such as Notch and Gli<sup>15, 19</sup>. Hence, the presence or absence of the insertion within the PTB domain could impact the interaction of the Numb proteins with E3 ligases and the targeted substrates<sup>15, 46</sup>. We found that the insert in the PTB domain did not affect the ability of the Numb proteins to interact with APP, in accord with a previous study showing that APP was

found in complex with all four mammalian Numb isoforms in cortical lysates<sup>24</sup>. The present study showed that Numb can bind directly to the YENPTY motif in the cytoplasmic domain of APP, an interaction that is not only required for the internalization of cell surface APP, but also for its subsequent transport and processing fate.

The accumulation of APP holoprotein did not correlate with a reduction of A $\beta$  secretion which supports the contention that the Numb proteins influence the trafficking of endogenous APP along endocytic rather than secretory routes. Additional data showed that inhibition of endocytosis by overexpression of a dominant-negative dynamin negates the observed effects of the Numb proteins on APP metabolism. Furthermore, treatment of the Numb clones with Brefeldin A to inhibit the transport of proteins from ER to Golgi did not show any effect on APP accumulation (data not shown) whereas lysosomal inhibitors restored steady state levels of APP in the LPTB-Numb clones.

The reduced sensitivity of the SPTB-Numb clones to inhibition of lysosomal degradation suggests that these Numb proteins may interfere with the transport of APP to the degradative pathway. Alternatively, we can not rule out the possibility that these Numb proteins play an active role in recycling internalized APP back to the cell surface. This notion is consistent with the increased amounts of released sAPP $\alpha$  and intracellular C83 generated by  $\alpha$ -secretase cleavage which occurs mainly at the cell surface. As dissociation of protein-protein complexes favors the recycling pathway, it remains to be elucidated whether the interaction of the Numb proteins and APP resulted in conformational changes that are differentially resistant to decreasing pH values within the endosomal pathway. Regardless of the underlying molecular mechanisms, our data suggest that the Numb proteins differentially alter the endocytic trafficking of APP by regulating the endosomal sorting of this protein either to the degradative or recycling

pathway. It will be interesting to examine whether the Numb proteins differentially affect the trafficking of other receptors with the conserved YENPTY motif such as TrkA, a tyrosine kinase receptor whose protein level and responsiveness to nerve growth factor (NGF) were shown to be differentially affected by the Numb proteins <sup>27</sup>.

Whether the Numb proteins are directly involved in the active transport of APP remains to be elucidated. Intracellular trafficking through the endocytic and recycling pathway are regulated by the small GTPase Rab proteins whose altered expression and activity has been linked to altered APP metabolism <sup>36, 47, 48</sup>. Rab5A upregulation is associated with enlarged early endosomes and intracellular accumulation of APP <sup>48</sup>. Altered Rab5A activity is responsible for the early abnormalities of the neuronal endocytic pathway that are directly related to a rise in A $\beta$  levels in brains of AD patients <sup>47, 48</sup>. Previous studies demonstrated that Numb interacts with Arf6 and EHD4 <sup>49</sup>, proteins that have been associated with the recycling of plasma membrane proteins internalized by clathrin-dependent and clathrin-independent endocytic routes <sup>50</sup>. Impairments in the sorting pathway could also account for the intraneuronal A $\beta$  accumulation in the brains of APP mutant transgenic mice and human AD patients <sup>51</sup>. We found that level of Rab5A protein but not mRNA was elevated in the SPTB-Numb clones suggesting that altered Rab5A function in part correlates specifically with altered trafficking of APP. The mechanism(s) whereby expression of SPTB-Numb but not increases Rab5A protein level remains to be established.

At present, the factors that regulate the alternative splicing of the primary Numb transcript are not known. It has been shown that the four Numb isoforms are temporally regulated and implement distinct developmental functions <sup>37, 38</sup>. Ectopic expression of Numb isoforms lacking the PRR insertion promotes differentiation whereas those isoforms with the insertion direct proliferation. Indeed, the expression of LPRR-Numb isoforms that promote



proliferation peaks during the expansion of the neural progenitor pool but is downregulated during the course of neuronal development<sup>37, 38</sup>. The expression pattern of the Numb proteins also varies dramatically between different tissues and cultured cell lines suggesting that Numb isoforms may have different functions in different cell types. Our previous study demonstrated that Numb protein levels increased in A $\beta$  laden brain regions of a mouse model of AD<sup>26</sup>. In this study, we found for the first time that pathophysiological conditions can upregulate the expression of SPTB-Numb at the expense of LPTB-Numb. This finding raises the intriguing possibility that altered Numb expression is an early pathologic event that may be responsible for increased A $\beta$  production in patients with AD.

Although the exact function of APP is still not resolved, experimental evidence suggests several activities including synaptogenesis, neurite outgrowth, and cell survival in neurons<sup>1</sup>. All of these activities may potentially be affected by the presence of Numb proteins determining the processing fates of APP. Of particular note is that overexpression of SPTB-Numb in PC12 cells enhanced neurite outgrowth<sup>27</sup> and increased vulnerability to apoptotic stimuli by a mechanism dependent on the dysregulation of intracellular Ca<sup>2+</sup> homeostasis<sup>26, 27</sup>. How Numb modulates intracellular Ca<sup>2+</sup> homeostasis remains to be elucidated. The disruption in Ca<sup>2+</sup> signaling may be linked to altered APP metabolism<sup>1, 52</sup> suggesting the involvement of altered Numb function or expression in the genesis of the AD phenotype. Hence, perturbation of Numb expression may have important implications for AD pathogenesis.

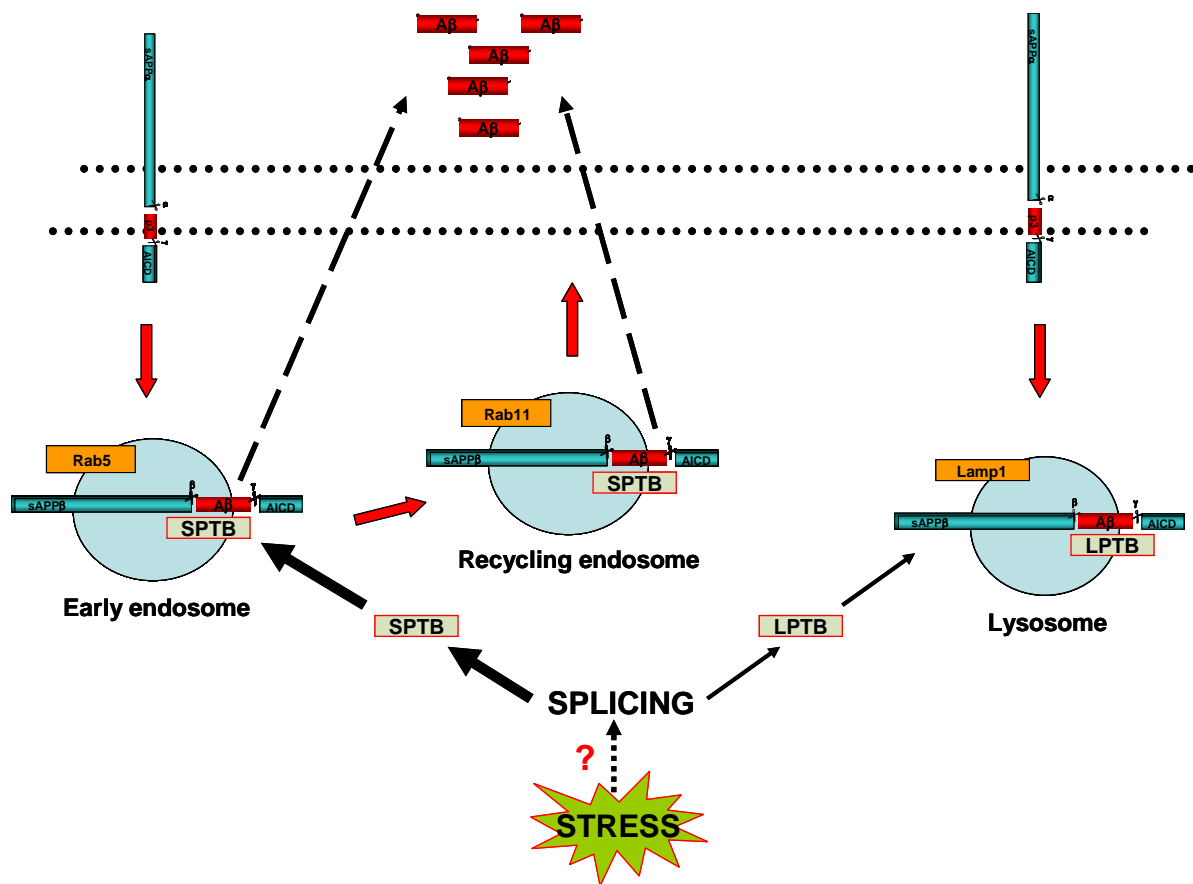


**Figure 11. Schematic diagram: Numb isoform-specific regulation of APP trafficking and A $\beta$  generation**

At the pro-neuronal PC12 cells, stress induces the alternative splicing of numb proteins that differ at the PTB domain favoring the upregulation of the SPTB isoform. Increases in the SPTB isoform of Numb regulates the endocytic trafficking of APP by preferentially shorting APP at the early and recycling endosomes. The accumulation of APP at these distinct endocytic compartments is accompanied by increased proteolytic processing by  $\beta$ - and  $\gamma$ - secretases and increased generation of A $\beta$  at the condition media.

## **CHAPTER II**

### **EFFECTS OF NUMB ISOFORMS ON NOTCH-DEPENDENT UPREGULATION OF TRPC6 CALCIUM CHANNELS**

#### *Introduction*

Numb was first identified in *Drosophila* as an asymmetrically localized protein involved in neural development<sup>10, 53</sup>, playing a key role in maintaining neural progenitor cells and preventing premature neuronal differentiation<sup>54</sup>. Notch is a type-I cell surface receptor that regulates cell fate decisions during neurogenesis<sup>55</sup>. Numb accomplishes its effects by antagonizing Notch signaling pathways<sup>56, 57</sup> via a mechanism that may involve Numb-mediated ubiquitination of Notch and subsequent degradation of Notch intracellular domain (NICD)<sup>58</sup>. Mammalian homologues of Numb have been identified suggesting an evolutionary conserved function of Numb<sup>54, 59-62</sup>. During mouse cortical neurogenesis, Numb is also asymmetrically localized, suggesting its potential role in the mammalian nervous system<sup>61</sup>. However, Numb is also expressed in many adult tissues, suggesting that its functions are not limited to neurogenesis<sup>57, 60</sup>. Structurally, Numb possesses an N-terminus phosphotyrosine binding (PTB) domain<sup>63</sup>, a proline-rich C-terminus region (PRR) containing SH-3 domain binding sites<sup>60</sup>, and an Eps15 homology (EH) domain binding motif<sup>64</sup>. Mammalian Numb is expressed in four isoforms differing in the length of the PTB (lacking or containing an 11 amino acid insert) and PRR (lacking or containing a 48 amino acid insert) domains<sup>59</sup>. Numb proteins containing an insertion in the PRR region (LPRR) promote proliferation of neural crest cells, while those lacking the insert (SPRR) appear to mediate neural differentiation<sup>65</sup>. These results suggest that the functions of Numb proteins may be isoform-specific and should be studied separately. PC12 cells stably

expressing the Numb isoform that is lacking the PTB insert (SPTB-Numb) stimulate NGF-induced differentiation and enhance apoptosis induced by NGF deprivation compared to cells that stably express the isoform with the PTB insert (LPTB-Numb)<sup>27</sup>. The role of PTB isoforms in cell fate decisions has been further supported by finding where the SPTB-Numb exhibit enhanced elevations of intracellular concentration of calcium ( $[Ca^{2+}]_i$ ) and increased cell death sensitivity in response to long-term exposure to amyloid- $\beta$  peptide ( $A\beta$ )<sup>26</sup>. The mechanism by which Numb modifies calcium homeostasis in SPTB-Numb is not clear, but considering the enhanced calcium responses to bradykinin, a known  $IP_3$  activator, it may involve enhanced release of calcium from endoplasmic reticulum (ER) stores<sup>26</sup>.

The critical role of calcium in many diverse cellular processes including muscle contraction, cell death and proliferation, signal transduction and transcriptional regulation has been established<sup>66</sup>. Calcium is an important intracellular messenger that mediates many physiological responses in neurons<sup>67</sup>. During normal physiological states, calcium signaling is initiated by transient increases in  $[Ca^{2+}]_i$  that emerge either by calcium entry into the cell from the extracellular space and/or by calcium release from the intracellular stores (i.e. ER),<sup>68</sup>. However, ample data suggest that perturbations of calcium homeostasis are involved in the pathogenesis of several neurodegenerative disorders and stroke<sup>69</sup>. A variety of different classes of calcium channels are found in the plasma membrane, which open in response to voltage-, second messenger-, receptor-, or store-operated mechanisms<sup>70</sup>. The transient receptor potential canonical (TRPC) calcium channels are one of the seven members of the TRP superfamily which are further divided into four subfamilies on the basis of sequence homology: TRPC1, TRPC2, TRPC3/6/7 and TRPC4/5<sup>71</sup>. TRPC channels are non selective cation channels that are activated in response to receptor- or store-operated signals including ER calcium store depletion<sup>72</sup>. More

specifically, TRPC6 can be directly activated by diacylglycerol (DAG) produced by receptor-activated phospholipase C (PLC) without any involvement of store-operated mechanisms <sup>73</sup>. Store-operated calcium entry (SOCE) can be triggered by any process that empties the intracellular stores of calcium (i.e. endoplasmic reticulum), regardless of the mechanism by which store depletion is accomplished <sup>74, 75</sup>. Despite the established role of TRPC6 as a receptor-operated channel, in pulmonary artery smooth cells, TRPC6 is upregulated in response to chronic hypoxia enhancing SOCE <sup>76</sup>. Accordingly, ER store depletion with thapsigargin induced translocation of TRPC6 channels to the plasma membrane <sup>77</sup>. Interestingly, functional TRPC6 assembles into homo- and heterotetramers including other members of the TRPC3/6/7 <sup>78</sup>, suggesting that supra-molecular complexes with other adaptor proteins may be present. For example, in PC12 cells a TRPC6 multiprotein complex is present containing protein kinase C (PKC), FK-506-binding protein-12kDa (FKBP12) and calcineurin /calmodulin <sup>79</sup>. The physiological role of TRPC6 is largely unknown but growing evidence suggests its involvement in various pathological conditions. Six mutations in TRPC6 gene are linked to the human kidney disease focal and segmental glomerulosclerosis (FSGS) <sup>80, 81</sup>. Three of these mutation result in a gain of function and therefore enhance TRPC6 signaling resulting in a pathogenic calcium overload leading to dysregulation and cell death <sup>81</sup>. Altered expression and function of TRPC6 channels has also been involved in the development of hypoxic <sup>82</sup> and idiopathic <sup>83</sup> pulmonary artery hypertension, angiotensin-induced cardiac hypertrophy <sup>84</sup>, Duchenne muscular dystrophy <sup>85</sup>, and Alzheimer's disease <sup>86</sup>. Despite the dispute about the modes of TRPC6 activation, the signaling events leading to its transcriptional control are not well understood.

Notch is a type-I transmembrane receptor present at the plasma membrane as a heterodimer (**Fig. 12**). Notch heterodimerization occurs in the trans-Golgi by a furin-like

convertase, during the secretion process<sup>87-89</sup>. Notch consists of an ectodomain known as NECD (Notch extracellular domain) linked non-covalently to the Notch transmembrane region (NTM)<sup>90</sup>. At the cell surface, Notch can interact with one of its ligands expressed in a neighboring cell and get activated<sup>91</sup>. In mammals, there are four Notch genes and five genes encoding ligands, three Delta-like and two Jagged<sup>92, 93</sup>. This interaction renders NTM sensitive to cleavage by extracellular metalloproteases of the ADAM/TACE (a desintegrin and metallopeptidase/tumor necrosis  $\alpha$  converting enzyme) family<sup>94-96</sup>. Subsequently, the remaining membrane Notch fragment undergoes proteolytic cleavage by a  $\gamma$ -secretase protein complex releasing NICD<sup>97-100</sup>. NICD translocates to the nucleus where it acts as a co-activator inducing transcriptional activation of its target genes<sup>99, 101</sup>.

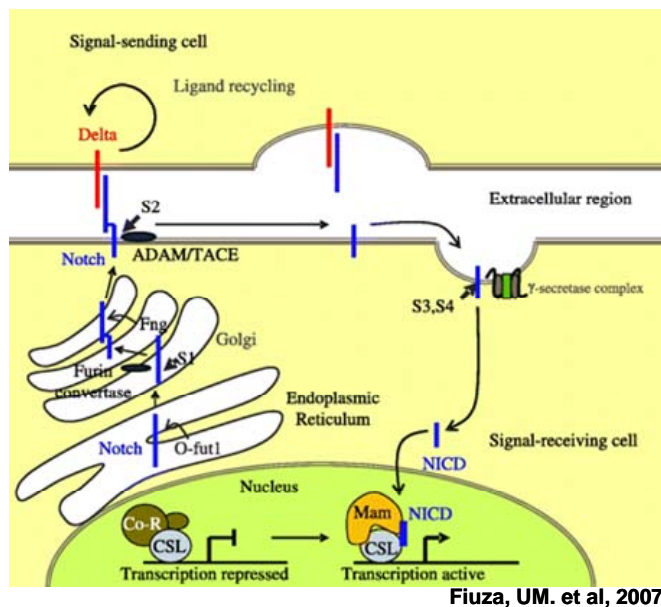


**Figure 12. Notch signaling activation**

Notch signaling affects cell fate decisions by critically influencing cell proliferation, differentiation, and apoptosis<sup>102</sup>. In *Drosophila*, lack of functional Notch showed an increase number of neuroblasts at the expense of epidermal precursors<sup>103</sup>. The functions of Notch,

however, are not restricted to neurogenesis but also involved in the development of other tissues like vessels, thymus, somite, central nervous system, heart, kidney and hematopoietic cells<sup>104-113</sup>. These functions of Notch are accomplished by tight regulation of its signaling activity that solely depends on the generation of NICD and/or its nuclear concentration<sup>98</sup>. However, the mechanism and conditions by which NICD is generated are of great importance and uncover connections between Notch trafficking and signaling activity<sup>114</sup>. As previously discussed, Numb is a membrane associated protein that inhibits Notch signaling. Numb is acting upstream of the  $\gamma$ -secretase by physically interacting with Notch and  $\alpha$ -adaplin, a component of the AP2 clathrin-adaptor complex<sup>115</sup>, suggesting that Numb may affect the endocytic fate of Notch. Alternatively, Numb interacts with the E3 ubiquitin ligase AIP4/Itch to promote ubiquitination, endocytosis and degradation of Notch1<sup>58</sup>. We have shown that Numb affects the endocytic trafficking and proteolytic fate of APP in an isoform specific manner (Kyriazis GA, et al. 2008). More specifically, the SPTB-Numb induced the accumulation of APP in the early endosomal and recycling compartments accompanied by enhanced proteolytic processing and generation of A $\beta$ . Due to the striking processing similarity between Notch and APP it is conceivable that Numb may also affect Notch endocytic fate in an isoform specific manner therefore affecting the generation of NICD.

Here we show that SPTB-Numb increase the expression of TRPC6 calcium channels and enhance SOCE compared to LPTB-Numb. SPTB-Numb mediate these transcriptional effects on TRPC6 by a mechanism that enhances Notch signaling. Furthermore, neural cells subjected to serum deprivation also enhance Notch activity inducing TRPC6 upregulation, effects that are preceded by a selective upregulation of the SPTB Numb isoform in expense of the LPTB one. In contrast, LPTB-Numb subjected to serum deprivation failed to increase Notch signaling or

TRPC6 expression, conferring protection from cell death. Taken together, these results suggest an isoform specific role of Numb in modulating calcium homeostasis by a mechanism that involves Notch-mediated transcriptional regulation of TRPC6 calcium channels.



## ***Materials and methods***

### ***Antibodies and reagents***

The polyclonal antibodies to the following protein were obtained: Rab5a (Santa Cruz), actin (Sigma), Notch1-M20 and Notch1-G20 (Santa Cruz), TRPC6 (Chemicon), TRPC-3,-6 (gifts from Dr. Schilling). Immunofluorescence-conjugated secondary antibodies (Alexa Fluor 488-conjugated goat anti-mouse and Alexa Fluor 594-conjugated rabbit anti-goat IgG) were obtained from Molecular Probes. Additional reagents included: Lipofectamine Plus reagent (Invitrogen), DAPT (Calbiochem),  $\beta$ -secretase inhibitor IV (Calbiochem), Thapsigargin (LC Laboratories).

### ***Cell culture and treatments***

PC12 cells were cultured in Dulbecco's Modified Eagle's Medium (DMEM) with 10% fetal bovine serum (FBS) (Invitrogen) and maintained at 37°C in a 5% CO<sub>2</sub> 95% air atmosphere. PC12 cells stably expressing Numb variants have been described previously<sup>27</sup>. Serum deprivation was accomplished by washing the cells with phosphate-buffered saline (PBS) and then maintained them in serum-free Locke's buffer<sup>26</sup> for designated times. DAPT (40 $\mu$ M) and  $\beta$ -secretase inhibitor IV (10 $\mu$ M) in Opti-MEM I was used to inhibit  $\gamma$ -secretase and  $\beta$ -secretase activity respectively. Thapsigargin (1mM) in Locke's Ca<sup>2+</sup>-free was used to inhibit SERCA. Jagged-1 peptide (15 $\mu$ M) in DMEM 1% FBS was used to activate Notch1 or appropriate scramble control (15 $\mu$ M) after washing cells 5 times with DMEM 1% FBS with 5 min incubations at 37°C in a 5% CO<sub>2</sub> 95% air atmosphere between washes.

### ***Intracellular calcium measurements***

Cells were cultured on poly-L-lysine-coated glass-bottomed chambers for 24-hr prior to intracellular  $\text{Ca}^{2+}$  experiments in DMEM + 10% FBS medium. Chambers were mounted onto the stage of an Olympus IX-50 fluorescent microscope equipped with an Hg excitation lamp and a Myocyte Photometry System (IonOptix, Milton, MA). Cells were superfused with DMEM saturated with 95%  $\text{O}_2$ -5%  $\text{CO}_2$  at 37° and containing 1.8 mmol/L  $\text{Ca}^{2+}$ . A 90% confluent area of 20-30 cells was chosen for each experiment. Cells were loaded with Indo-1 by incubation in Tyrode's solution containing (in mmol/L): 138 mM NaCl, 5.4 mM KCl, 1.8 mM  $\text{CaCl}_2$ , 1  $\text{MgCl}_2$ , 10 HEPES, 10 Glucose and 10  $\mu\text{mol/L}$  Indo-1 AM ester (Molecular Probes, Eugene, OR), pH=7.4, at room temperature for 35 min. After loading, oxygenated DMEM superfusate at 37° was returned for 10 min to wash-out unincorporated dye. Experimental protocols were performed in Locke's solution with  $\text{Ca}^{2+}$  (2.0mM), or in  $\text{Ca}^{2+}$ -free Locke's solution with EGTA (100 $\mu\text{M}$ ) saturated with 95%  $\text{O}_2$ -5%  $\text{CO}_2$  at 37°. The 405nm and 475nm emission of Indo-1 excited at 340nm was collected by a double-photometer unit, and  $\text{Ca}^{2+}$  ratio transients were recorded in Ion Wizard v4.44 (IonOptix). Fluorescence quench was recorded at 360 nm using  $\text{MnCl}_2$  ( $\text{Mn}^{2+}$  200 $\mu\text{mol/L}$ ). At the conclusion of all experiments, background numerator and denominator counts were measured from a cell-free region of the coverslip.

For the experimental procedure cells were equilibrated in  $\text{Ca}^{2+}$ -free Locke's for 9 min (in 15 sec intervals) and then thapsigargin (1mM) was added. Measurements were taken for 15min and until  $\text{Ca}^{2+}$  ratio readings plateau. Cells were then superfused with  $\text{Ca}^{2+}$  Locke's solution.

Measurements continued for 6min after  $\text{Ca}^{2+}$  peak was recorded. Ratiometric units were converted to intracellular  $\text{Ca}^{2+}$  concentrations by the Grynkiewicz equation <sup>116</sup>:

$$[\text{Ca}^{2+}] = K_d \beta (R - R_{\min}) / (R_{\max} - R)$$

Ionomycin  $\text{Ca}^{2+}$  salt (Sigma) (2  $\mu\text{mol/L}$  in DMEM) was applied before background measurements at the conclusion of experiments to obtain  $R_{\max}$  value. These values were pooled for each set of experiments of particular cell type and culture protocol. Ionomycin at higher concentrations was observed to cause morphological changes and loss of cell adherence, implying lethality. No significant change in  $R_{\max}$  was observed from 1-5  $\mu\text{mol/L}$ .  $R_{\min}$  value was the mean of background-subtracted ratios obtained from an experimental chamber without cells containing  $\text{Ca}^{2+}$ -free Locke's and 10  $\mu\text{M}$  Indo-1  $\text{Na}^+$  salt.

### ***Cell death assays***

Cells were plated on cover slips in 24-wells. Cells were washed with PBS and then treated with serum withdrawal medium for designated times. Then cells were washed twice with PBS and incubated for 15 minutes at 37°C with 2 $\mu\text{M}$  propidium iodide (PI) and 5 $\mu\text{g/ml}$  of Hoechst dye in PBS. Cells were washed twice with PBS and fixed with 4% paraformaldehyde for 1 hour at room temperature. Cover slips were mounted at microscope slides using DPX mountant for histology (Fluka) and visualized under a fluorescent microscope (Carl Zeiss). Cells were counted and the percent cell death was assessed using a ratio of PI stained cells to total Number of cells (Hoechst staining) in the field.

## ***siRNA***

Stably transfected PC12 cells with Numb SPTB-Numb were cultured as described above to 50% confluency. TRPC6 were knock downed using Stealth siRNA (Invitrogen) (TRPC6: AACAUUCCAAAGUCAAGCAUAUUCC), each with its complementary sequence or Stealth RNAi Negative control duplex (Invitrogen). Cells plated and transfected with 200nM of siRNA and Lipopfectamine 2000 (Invitrogen) in Opti-MEM I reduced medium without serum for 24-48 hours and then subjected to the experimental treatments described above.

## ***RNA isolation and Real-Time PCR***

Total RNA from cells grown in 60mm dishes was isolated using Trisol reagent (Invitrogen). RNA (2 $\mu$ g) was used to synthesize cDNA using Enhanced Avian HS RT-PCR Kit (SIGMA). Real time quantitative PCR was performed using an iCycler (BioRad). Amplification was performed in a final volume of 20  $\mu$ l, including cDNA from the reverse transcribed reaction, primer mixture (0.4  $\mu$ M each of sense and antisense primers), and 12.5  $\mu$ l 2x SYBR Green Master Mix (BioRad). The oligonucleotide primers are listed on Table 1. A serially diluted positive control sample was used to create a standard curve and determine the sensitivity and linearity of the assay. The standard amplification program included 40 cycles of two steps, each comprising heating to 95 °C and heating to 60 °C. Fluorescent product was detected at the last step of each cycle. In order to verify the purity of the products, a melting curve was produced after each run. To determine the relative quantization of gene expression, the comparative threshold cycle method ( $\Delta C_T$ ) was used<sup>117</sup>. Variation in RNA quantity and quality was controlled using GAPDH or 18S ribosome RNA as internal controls. To calculate a relative  $C_t$  for the target molecules

(TRPC channels) of interest the  $C_T$  of the control gene was subtracted from the  $C_T$  of the gene of interest to yield the  $\Delta C_T$ . The final mRNA levels were normalized according to their  $C_t$  values from the standard curves.

**Table 1. Oligonucleotide sequences of primers used for Real Time RT-PCR**

Target Gene	Accession Number	Orientation	Sequence (5'-3')
TRPC1	AF061266	Forward Reverse	CGACACCTTCCACTCGTTCA GCGCTAAGGAGAAGATGTACCAGA
TRPC2	NM017011	Forward Reverse	GTTCCAGTTTCTCTTCTGGACCAT CAGCATCGTCCTCGATCTTCT
TRPC3	AB022331	Forward Reverse	CATGCAGTGCAAAGACTTCGTAG TTCAGAATGGCTTCCACCTCTT
TRPC4	NM_080396	Forward Reverse	CTCTGCAGATATCTCTGGGAAGAAT CACGAGGCAGTATATGAATAAGAACTTT
TRPC5	AY064411	Forward Reverse	TGAAACCCTTCAGTCACTCTTCTG AGTAGCTCCCACAACTCCGTG
TRPC6	NM_053559	Forward Reverse	AGTGTACAGAATGCAGCCAGAAAC CAGCCCTTTGTAGGCATTGATC
TRPC7	XM_225159	Forward Reverse	CCCTTTAACCTGGTGCCGA TGGAGTTCAGCATGCCATT
18S	X01117	Forward Reverse	GTAACCCGTTGAACCCCAT CCATCCAATCGGTAGTAGCG
GAPDH	NM_017008	Forward Reverse	ACCCCTTCATTGACCTCAACT ATGCCAGTGAGCTTCCCCTCAGC
Numb	NM_133287	Forward Reverse	TCAAGAGGAATGCACATCTGTGAAG TTCATCCACAACCTCTGAGTCCATC
Numb-LPTB	NM_133287	Forward Reverse	GGAAGTTCTTCAAAGGCTTCTTTG TTCATCCACAACCTCTGAGTCCATC
Notch1	NM_001105721	Forward Reverse	TGGAGCTACCTGCACTGACTATC TCTCCTCGGAGCAGTTAGACC
HES-1	NM_024360	Forward Reverse	AAAGATAGCTCCCGGCATTC CCTCACACGTGGACAGGAA

## ***Results***

### ***SPTB-Numb is characterized by SOCE and increased expression of TRPC calcium channels***

We have previously shown that SPTB-Numb demonstrated significantly higher  $[Ca^{2+}]_i$  relative to vector (VT) and LPTB-Numb after treatment with bradykinin <sup>27</sup>, an agonist that induces calcium release from the ER <sup>118</sup>. In order to elucidate whether the bradykinin-evoked transient  $[Ca^{2+}]_i$  increase in SPTB-Numb is due to an enhanced ER calcium pool, VT, SPTB-Numb, and LPTB-Numb were treated with thapsigargin in calcium-free medium. Thapsigargin depletes the ER calcium pool by irreversibly inhibiting the sarcoplasmic/endoplasmic  $Ca^{2+}$ -ATPase pump (SERCA) <sup>119</sup>. SPTB-Numb showed increased calcium concentration after thapsigargin treatment compared to VT and LPTB-Numb, indicating that SPTB-Numb have enlarged ER calcium pool (**Fig 13.a**). Depletion of the endogenous calcium pool induces SOCE, via a mechanism that involves specific channels <sup>120</sup>. Following depletion of the ER calcium pool with TG, calcium (2 mM) was added to the medium to induce SOCE. SPTB-Numb demonstrated an enhanced SOCE compared to VT and LPTB-Numb (**Fig 13.a**). TRPC channels are the most likely candidates in mediating SOCE <sup>121</sup>, so we measured the expression levels of TRPC channels in neural cells stably expressing the Numb isoforms. VT express TRPC1 and moderate levels of TRCP3 under basal conditions. TRPC2, -4, -5, and -7 are either minimally expressed or undetected (**Fig 13.b**). Similar findings were observed in the LPTB-Numb. In contrast, in SPTB-Numb the expression levels of most TRPC channels were increased. Interestingly, the expression levels of TRPC3 and TRPC6 channels were 36-fold and 95-fold higher respectively in SPTB-Numb compared to VT (**Fig 13.b**).

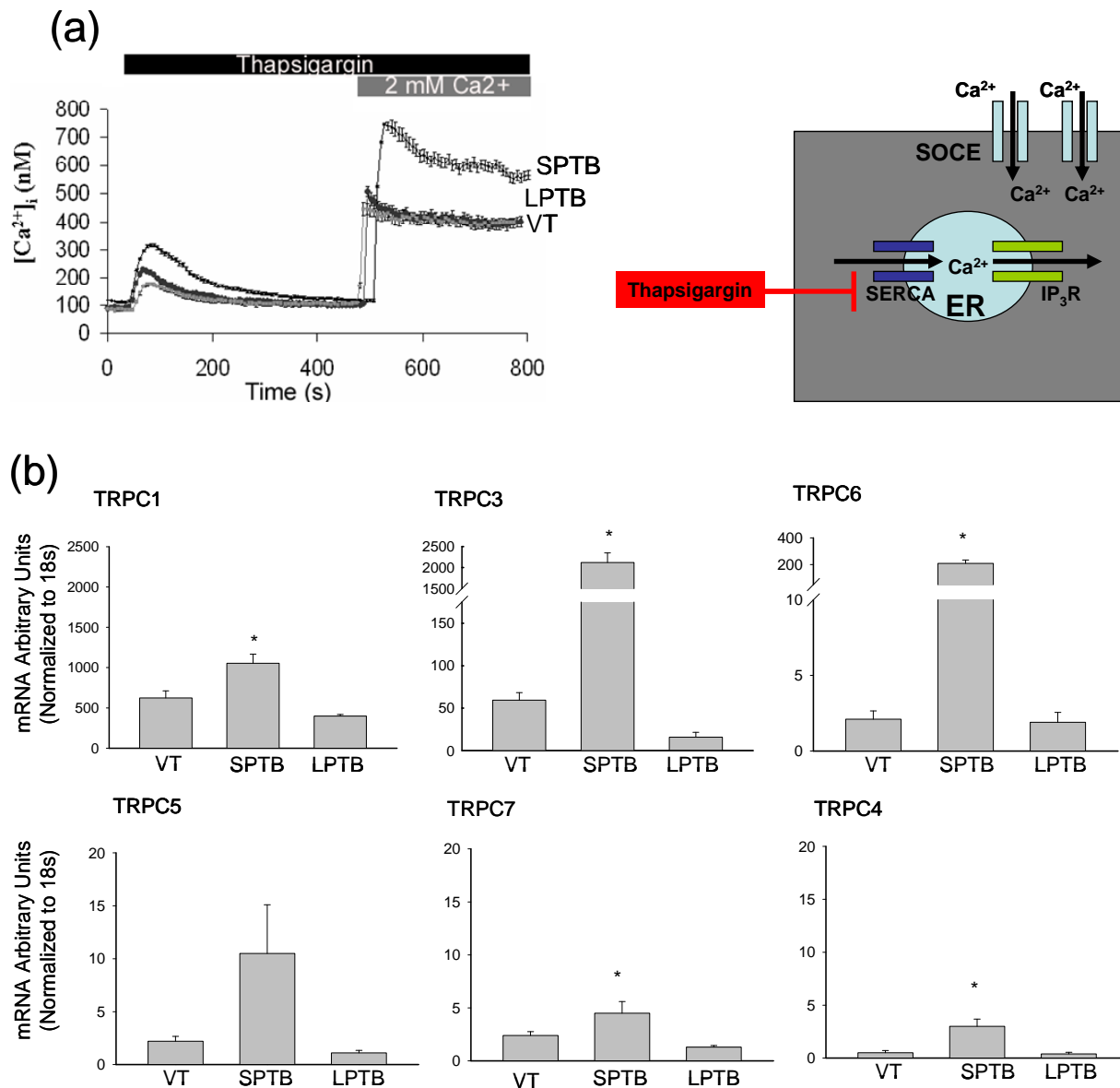


**Figure 13. Thapsigargin-induced SOCE and TRPC calcium channel expression.**

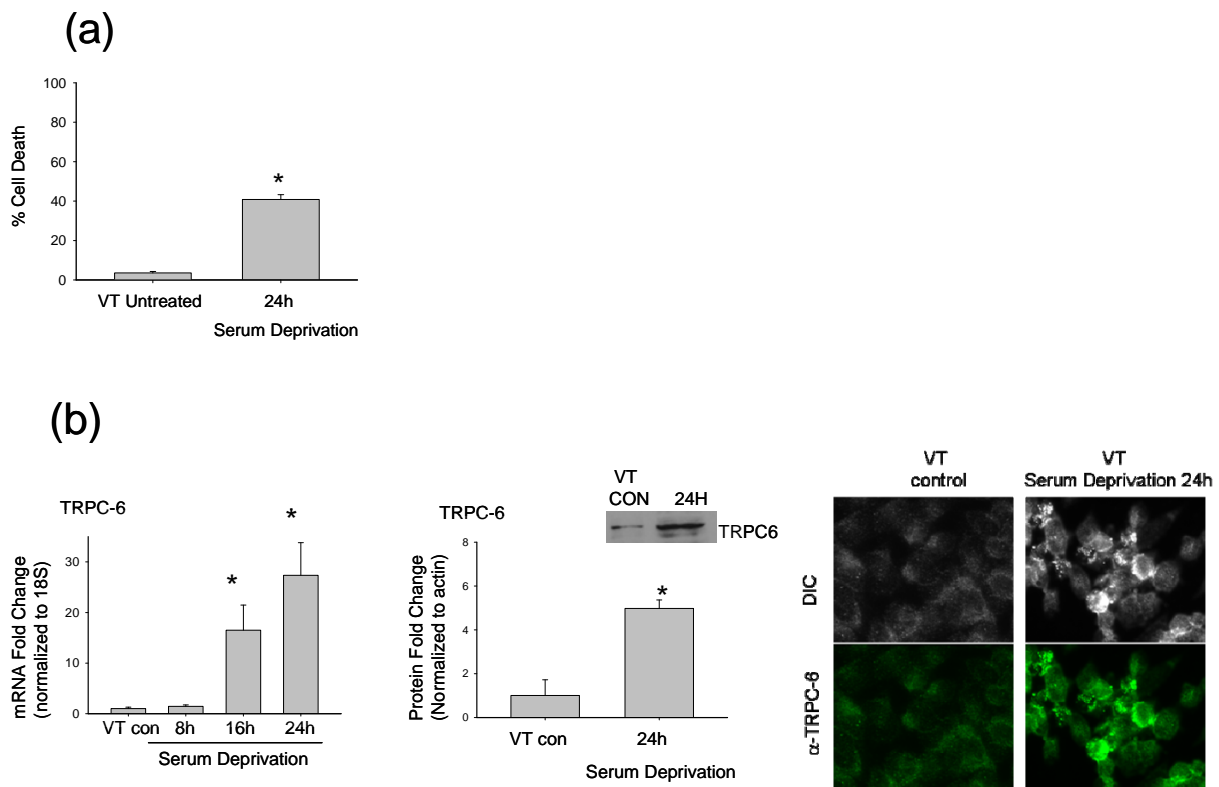
**(a)** Composite traces of  $[Ca^{2+}]_i$  as a function of time are shown. Cells were perfused with Locke's  $Ca^{2+}$ -free medium with  $100\mu M$  EGTA for 6 minutes. Thapsigargin ( $1mM$ ) was added and  $[Ca^{2+}]_i$  was recorded for 8 minutes. Cells were then perfused with Locke's  $Ca^{2+}$  ( $2mM$ ) and SOCE was recorded. **(b)** Relative expression levels of TRPC channels in the stable PC12 clones normalized to 18s mRNA ( $n=6$ ;  $*p<0.01$  vs. VT and LPTB-Numb). Data are mean  $\pm$  SEM.

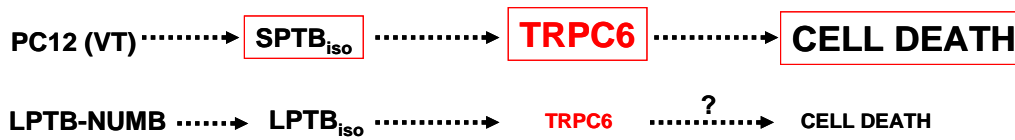
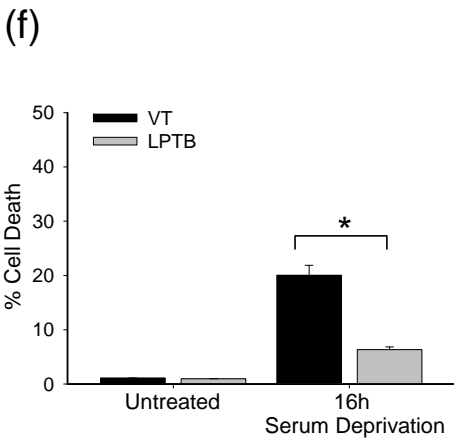
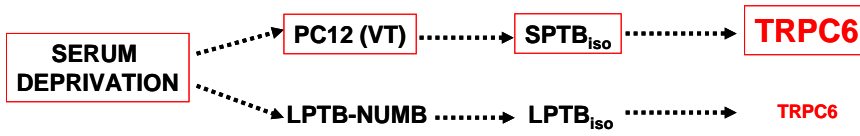
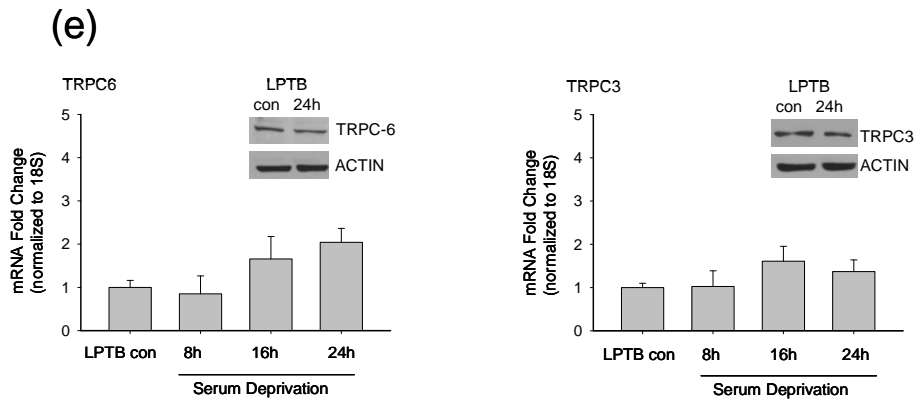
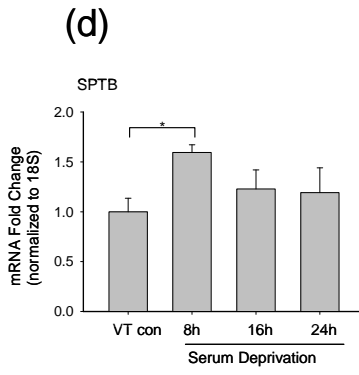
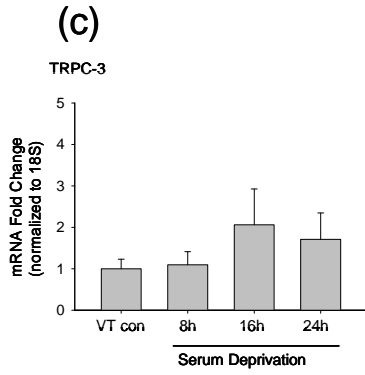
### ***Serum deprivation-induced cell death is mediated by TRPC6 upregulation***

We have previously shown that SPTB-Numb exhibited increased susceptibility to cell death upon serum deprivation <sup>27</sup>. Since SPTB-Numb were found to have high expression levels of TRPC3 and TRPC6 we tested whether the increased vulnerability of these clones is mediated by these channels. PC12 cells were subjected to serum deprivation for various time points (8, 16, and 24 hours) and the expression levels of TRPC3 and TRPC6 were measured. Cell death was significantly increased after 24h of serum deprivation compared to untreated control ( $40.8\pm 0.46\%$  vs.  $3.6\pm 0.70\%$ ) (**Fig 14.a**). TRPC6 mRNA was increased at 16h ( $16.51\pm 4.96$ -fold) and 24h ( $27.32\pm 6.46$ -fold) of serum deprivation compared to untreated control (**Fig 14.b; left panel**). These mRNA changes in TRPC6 were accompanied by increases in the protein levels ( $4.97\pm 0.38$ -fold) (center panel), as well as by accumulation of TRPC6 at the cell membrane (right panel). No significant upregulation of TRPC3 mRNA was observed (**Fig 14.c**). Interestingly, the serum deprivation-induced upregulation of TRPC6 in PC12 cells was preceded (at 8h) by a significant upregulation ( $1.59\pm 0.07$ -fold) of the SPTB spliced isoform of Numb (**Fig 14.d**). This finding is consistent with the upregulation of TRPC6 observed in SPTB-Numb. In order to further elucidate the significance of the SPTB isoform of Numb in the regulation of TRPC6 channel, we tested whether similar changes can be observed in the LPTB-Numb, where the LPTB isoform of Numb is overexpressed. No significant upregulation of mRNA or protein levels of either TRPC6 or TPRC3 was observed (**Fig 14.e**), suggesting that the presence of the SPTB-Numb isoform may be necessary for such changes to occur. Then we tested whether the absence of TRPC6 upregulation in LPTB-Numb confers protection against serum deprivation. Indeed, cells death was significantly lower in LPTB-Numb ( $6.34\pm 0.005\%$ ) compared to VT ( $20.43\pm 0.048\%$ ) after 16h of serum deprivation (**Fig 14.f**). Moreover, to further confirm the role



of TRPC6 upregulation in serum deprivation-induced cell death, we used siRNA to knock down TRPC6 and test whether it will decrease the vulnerability of PC12 cells. Treatment with siRNA (siTRPC6) successfully reduced the mRNA levels of TRPC6 ( $0.53\pm 0.15$ -fold) compared to scramble control, after 24h of serum deprivation (**Fig 14.g**). Cell death was significantly reduced in PC12 cells treated with siTRPC6 ( $37.71\pm 4.56\%$ ) compared to scramble ( $67.15\pm 5.24\%$ ) after 24h of serum deprivation (**Fig 14.h**). These results suggest that, at least in PC12 cells, TRPC6 upregulation is implicated in the serum deprivation-induced cell death, and that the SPTB isoform of Numb may mediate its upregulation.





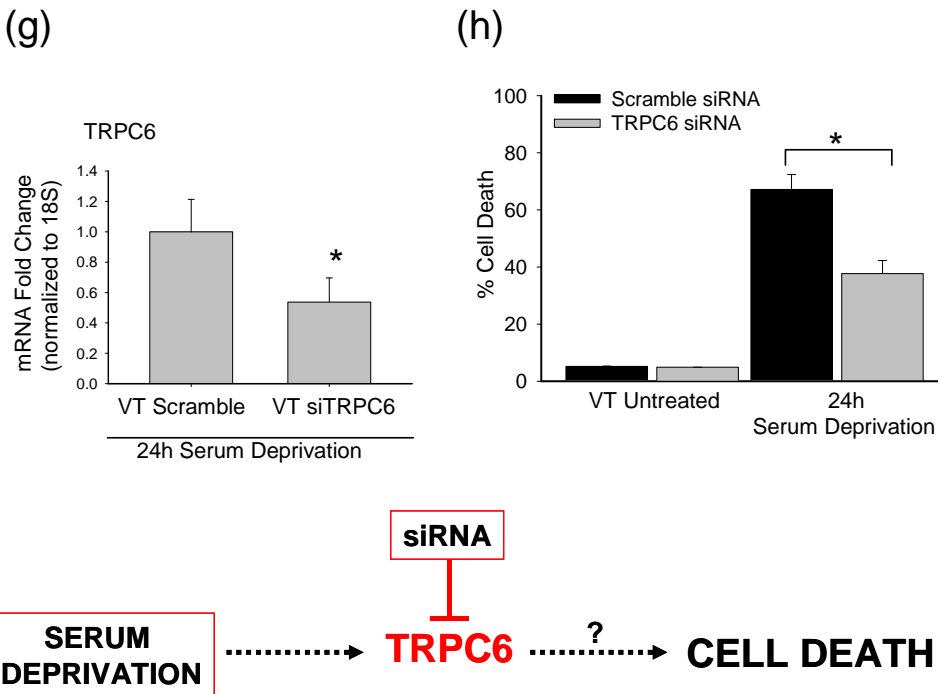


**Figure 14. TRPC6 upregulation mediates serum deprivation-induced cell death in PC12 cells via a mechanism that involves the SPTB isoform of Numb**

(a) Percent (%) cell death in VT after 24h of serum deprivation (n=3; \*p<0.0001). (b) Fold change in TRPC6 mRNA (left panel; n=6) and protein levels (center panel; n=3), and TRPC6 cellular localization (right panel) in VT after 24h of serum deprivation compared to untreated control (\*p<0.01). (c) Fold change in TRCP3 mRNA levels in VT after serum deprivation compared to untreated controls (n=6). (d) Fold change in the SPTB isoform of Numb mRNA levels in VT after serum deprivation compared to untreated controls (n=6; \*p=0.003). (e) Fold change in TRPC3 and TRPC6 mRNA and protein levels in LPTB-Numb after serum deprivation compared to untreated controls (n=6). (f) Percent (%) cell death in VT and LPTB-Numb before and after serum deprivation (n=3; \*p<0.0001). (g) Fold change in TRPC6 mRNA levels in VT treated with scramble or siRNA directed to TRPC6 (siTRPC6) after 24h of serum deprivation (n=3; \*p=0.015). (h) Percent (%) cell death in VT treated with scramble or siTRPC6 before and after 24h of serum deprivation (n=3; \*p=0.013). Data are mean  $\pm$  SEM.

### ***Notch signaling is enhanced in SPTB-Numb***

Numb is involved in asymmetric cell division during embryogenesis by antagonizing Notch signaling<sup>56, 122</sup>. It has been suggested that the effects of Numb in regulating Notch-mediated signaling may be isoform-specific<sup>123</sup>. As such, we tested whether Notch signaling is differentially affected by overexpressing Numb isoforms. Notch is activated by cleavage and release of its intracellular domain (NICD), which then translocates to the nucleus regulating the transcriptional activity of target genes<sup>101, 124</sup>. Protein levels of NICD were increased in SPTB-Numb (0.98±0.02) compared to VT (0.77±0.009) and LPTB-Numb (0.61±0.01) (**Fig 15.a**). NICD was largely localized into the nucleus of SPTB-Numb suggesting increased transcriptional activity (**Fig 15.b**). A well reported downstream transcriptional target gene of NICD is Hairy/Enhancer of Split-1 (HES-1)<sup>103</sup>. In order to test whether the accumulation of NICD in the nucleus of SPTB-Numb clones is accompanied by increased transcriptional activity the relative levels of HES-1 mRNA were assessed. We found increased levels of HES-1 expression in SPTB-Numb (321.2±39.40) compared to VT (49.00±9.31) and LPTB-Numb (42.02±2.90) (**Fig 15.c**), confirming that Notch signaling in SPTB-Numb is enhanced. Then, we tested whether the increased activity of Notch in SPTB-Numb is due to altered expression of Notch1 gene, or enhanced  $\gamma$ -secretase activity. Neither Notch1 expression (**Fig 15.d**), nor the activities of  $\gamma$ -secretase (**Fig 15.e**) were different in SPTB-Numb compared to VT and LPTB-Numb. Considering that Numb promotes ubiquitination, endocytosis and degradation of Notch1<sup>58</sup> we speculated that Numb isoforms may differentially affect the endocytic fate of Notch. In SPTB-Numb, Notch1 co-localized with Rab5a, a marker of early endosome formation (**Fig 15.f; left column**). No such co-localization between Notch1 and Rab5a was observed in LPTB-Numb (**Fig**

**15.f; right column).** These data suggest that SPTB-Numb may alter Notch activity by promoting its accumulation in distinct endocytic compartments.

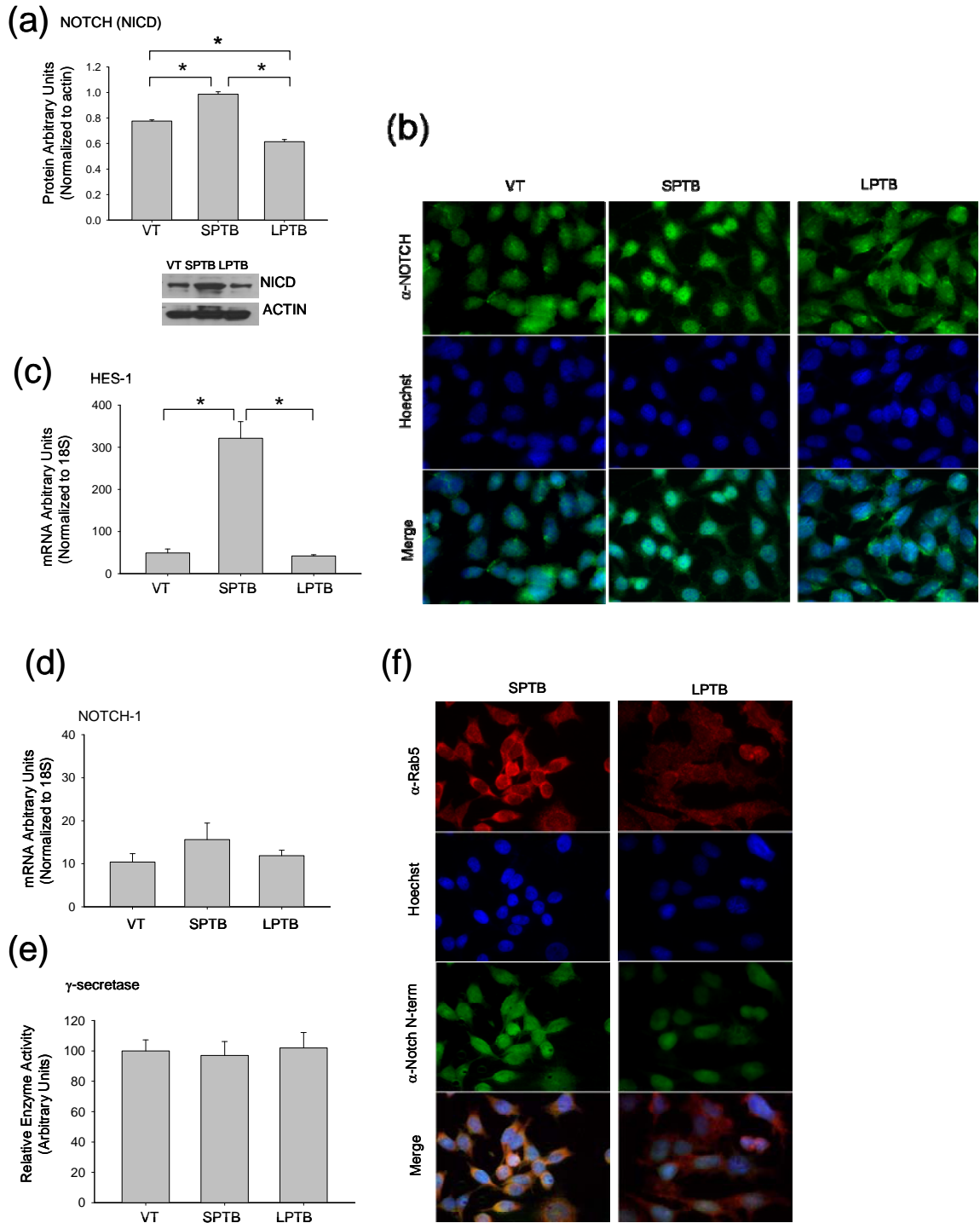


**Figure 15. Notch signaling is enhanced in SPTB-Numb**

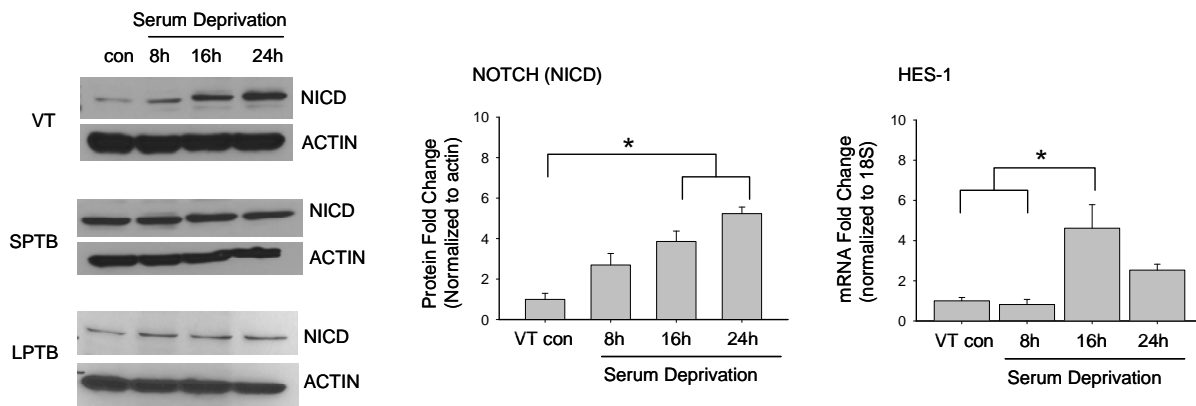
(a) Protein levels of the active form of Notch (NICD) in vector (VT), SPTB-Numb and LPTB-Numb respectively (n=3; \*p<0.001). (b) Cellular localization of Notch-NICD (green) in VT, SPTB-Numb and LPTB-Numb with Hoechst nuclear staining (blue). Merge of Notch and Hoechst nuclear staining (bottom panel). (c) HES-1 and (d) Notch1 mRNA expression in VT, SPTB-Numb and LPTB-Numb respectively (n=3; \*p<0.001). (e) Relative  $\gamma$ -secretase activities in VT, SPTB-Numb and LPTB-Numb respectively. (f) Cellular localization of Rab5 (red) and Notch (green) with Hoechst nuclear staining (blue). Merge of Rab5, Notch, and Hoechst nuclear staining (bottom panel). Data are mean  $\pm$  SEM.

### ***Serum deprivation increases Notch signaling in PC12 cells***

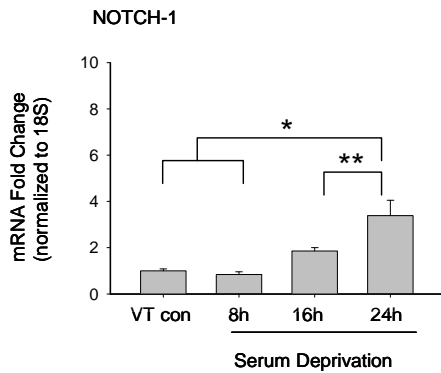
Since Notch signaling is enhanced in cell overexpressing SPTB-Numb and TRPC6 upregulation mediates the serum deprivation-induced cell death in PC12 cells, we tested whether serum deprivation would also activate Notch signaling in PC12 cells. We subjected all clones to serum deprivation for various time points and measured the protein levels of NICD. NICD protein was significantly increased in VT clones after 16 h ( $3.86\pm 0.51$ -fold) and peaked at 24 h ( $5.23\pm 0.32$ -fold) of serum deprivation (**Fig 16.a; center panel**). These changes in NICD protein induced a significant mRNA upregulation of HES-1 ( $4.61\pm 1.17$ -fold) after 16 h of serum deprivation (**Fig 16.a; right panel**). No significant NICD protein upregulation was observed in SPTB-Numb or LPTB-Numb upon serum deprivation (**Fig 16.a; left panel**). It has been suggested that Notch1 signaling is required to sustain *Notch1* gene transcription via a positive feedback loop<sup>125</sup>. Consequently, we tested whether the NICD protein upregulation in VT is due to enhanced transcriptional regulation of Notch1, or increased proteolytic cleavage of Notch by  $\gamma$ -secretases. The mRNA level of Notch1 was increased at 16 h ( $1.86\pm 0.14$ -fold) and peaked at 24 h ( $3.38\pm 0.67$ -fold) of serum deprivation, partly explaining the protein upregulation of NICD

(Fig 16.b). In contrast, no significant increases in Notch1 mRNA were detected in LPTB-Numb consistent with the absence of NICD changes (Fig 16.c). Moreover, serum deprivation induced a time-dependent cellular redistribution of NICD to the nucleus of VT (Fig 16.d), supporting the aforementioned increases in NICD protein and Notch transcriptional activity. Collectively, these data suggest that the TRPC6 upregulation in SPTB-Numb and in response to serum deprivation may be mediated by a mechanism that involves increased Notch activity.

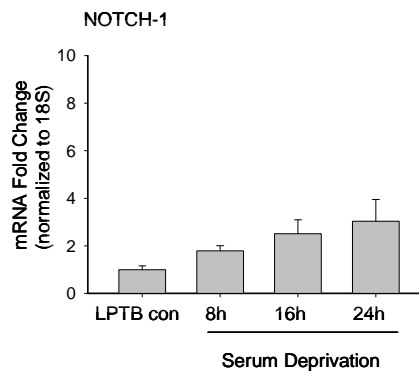
(a)



(b)



(c)



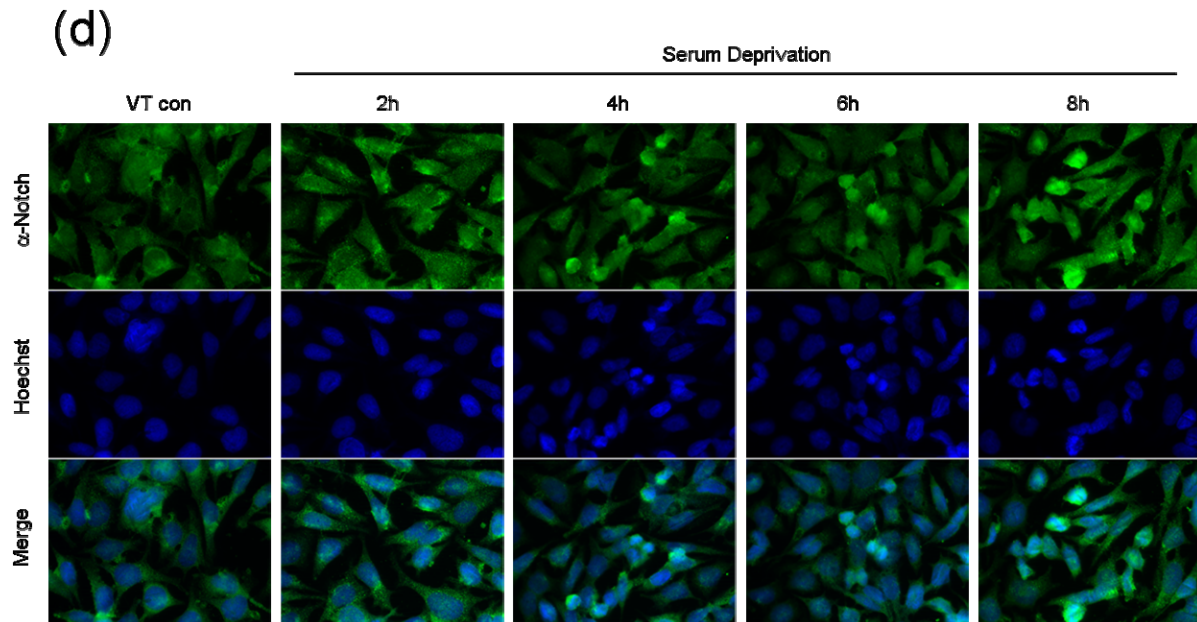


**Figure 16. Serum deprivation increases Notch signaling in PC12 cells**

Cells were subjected to serum deprivation or untreated control for various times. **(a)** Western blot of NICD levels with actin as loading control in VT, SPTB-Numb and LPTB-Numb (left panel). Fold change of NICD protein in VT (n=3; \*p<0.005) (center panel). Fold change of HES-1 mRNA in VT (n=3; \*p<0.007) (right panel) **(b-c)** Fold change of Notch1 mRNA in VT and LPTB-Numb (n=3; \*p=0.001, \*\*p=0.031). **(d)** Time course of NICD expression and nuclear redistribution (green) in VT with nuclear staining (blue). Merge of  $\alpha$ -Notch and Hoechst nuclear staining (bottom panel). Data are mean  $\pm$  SEM.

### ***Suppression of Notch signaling by a $\gamma$ -secretase inhibitor attenuates TRPC6 expression in SPTB-Numb***

NICD is released upon proteolytic cleavage by a protein complex that contains  $\gamma$ -secretase activity<sup>97, 98</sup>. As such, we tested whether a known  $\gamma$ -secretase inhibitor, N-[N-(3,5-difluorophenacetyl-L-alanyl)]-(S)-phenylglycine t-butyl ester (DAPT), can attenuate the increased expression of TRPC6 in SPTB-Numb. DAPT (40 $\mu$ M) treatment for 24 h was adequate



to decrease the relative expression of HES-1 mRNA ( $321.2 \pm 39.4$  vs.  $247.8 \pm 35.1$ ) in SPTB-Numb consistent with reduced proteolytic release of NICD and attenuated transcriptional activity of its downstream target genes (**Fig 17.a**). Interestingly, TRPC6 mRNA expression was also reduced ( $241.5 \pm 29.9$  vs.  $102.5 \pm 34.6$ ) in SPTB-Numb, but no effects were observed in the mRNA expression of TRPC3 (**Fig 17.b**). These transcriptional changes were also accompanied by reduced TRPC6 protein levels ( $0.51 \pm 0.01$ -fold) in SPTB-Numb compared to untreated control (**Fig 17.c; right panel**). No changes at the protein levels of TRPC3 were observed (**Fig 17.c; left panel**). These data demonstrate that  $\gamma$ -secretase inhibition selectively attenuates the transcriptional upregulation of TRPC6 in SPTB-Numb, suggesting an involvement of Notch signaling. Several substrates other than Notch are cleaved by  $\gamma$ -secretase, releasing their intracellular domain which, in most cases, contains biologically relevant properties<sup>126</sup>. APP, a well characterized substrate of  $\gamma$ -secretase, is cleaved by  $\beta$ - and  $\gamma$ -secretases releasing A $\beta$  at the extracellular space and the transcriptionally active APP intracellular domain (AICD) in the cytoplasm<sup>127</sup>. We have shown that Numb regulates APP trafficking and processing, so we tested whether a  $\beta$ -secretase inhibitor could also attenuate TRPC6 upregulation in SPTB-Numb. Treatment with the  $\beta$ -secretase inhibitor IV ( $10 \mu\text{M}$ ) for 24 h did not effect TRPC3 or TRPC6 expression (**Fig 17.d**). These results are consistent with the notion that the effects of DAPT on TRPC6 attenuated expression are mediated by inhibition of Notch signaling and not by APP.

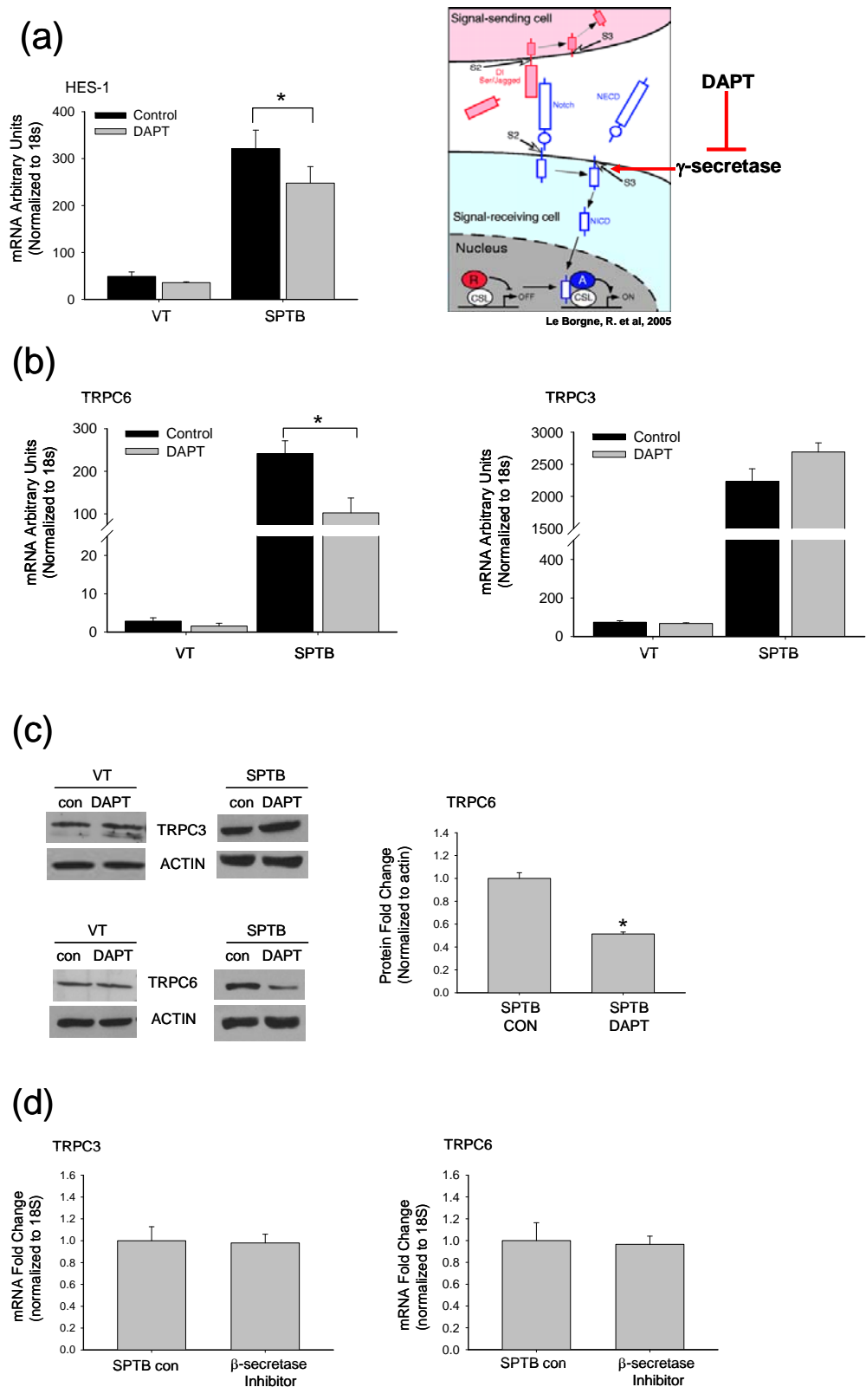


**Figure 17. Notch inhibition abrogates TRPC6 upregulation in SPTB-Numb**

Vector (VT) and SPTB-Numb were treated with DAPT (40 $\mu$ M), or  $\beta$ -secretase inhibitor IV (10 $\mu$ M) for 24h. **(a)** HES-1 mRNA expression levels in VT and SPTB-Numb before and after DAPT treatment (n=6; \*p=0.007). **(b)** TRPC6 and TRPC3 mRNA expression levels in VT and SPTB-Numb before and after DAPT treatment (n=6; \*p=0.01). **(c)** Western blot of TRPC3 and TRPC6 protein levels in VT and SPTB-Numb before and after DAPT treatment (left panel). Fold change of TRPC6 protein in SPTB-Numb before and after DAPT treatment (right panel) (n=3; \*p=0.037). **(d)** TRPC6 and TRPC3 mRNA expression levels in VT and SPTB-Numb before and after  $\beta$ -secretase inhibitor treatment (n=3). Data are mean  $\pm$  SEM.

### ***Jagged1- mediated activation of Notch induces TRPC6 upregulation in PC12 cells***

Since inhibition of Notch signaling attenuated TRPC6 expression in SPTB-Numb we set to investigate whether activation of Notch signaling can confer the opposite effects and upregulate the transcription of TRPC6 in PC12. In mammals, Jagged-1 is a well characterized Notch ligand, which upon binding to Notch receptors induces the release of NICD and therefore Notch signaling activation<sup>128</sup>. PC12 cells were treated with either rat Jagged-1 peptide (15 $\mu$ M), or a scramble control peptide (15 $\mu$ M) for various time points and the mRNA expression levels of HES-1, TRCP3, TRPC6 and SPTB isoform of Numb were measured. Jagged-1 peptide activated Notch signaling by inducing HES-1 mRNA expression after 4 h of treatment (1.85 $\pm$ 0.10-fold) compared to scramble control peptide (**Fig 18.a**). Similarly, Jagged-1 peptide treatment induced TRPC6 mRNA at 4 h (11.83 $\pm$ 4.11-fold) compared to scramble control peptide (**Fig 18.b**). No effects on TRPC3 mRNA expression were detected (**Fig 18.c**). These results suggest that Notch selectively upregulates the expression of TRPC6 in PC12 cells. Activation of Notch signaling did

not affect the expression of SPTB isoform of Numb (**Fig 18.d**), suggesting that the Notch-mediated transcriptional regulation of TRCP6 can occur independently of Numb functions.

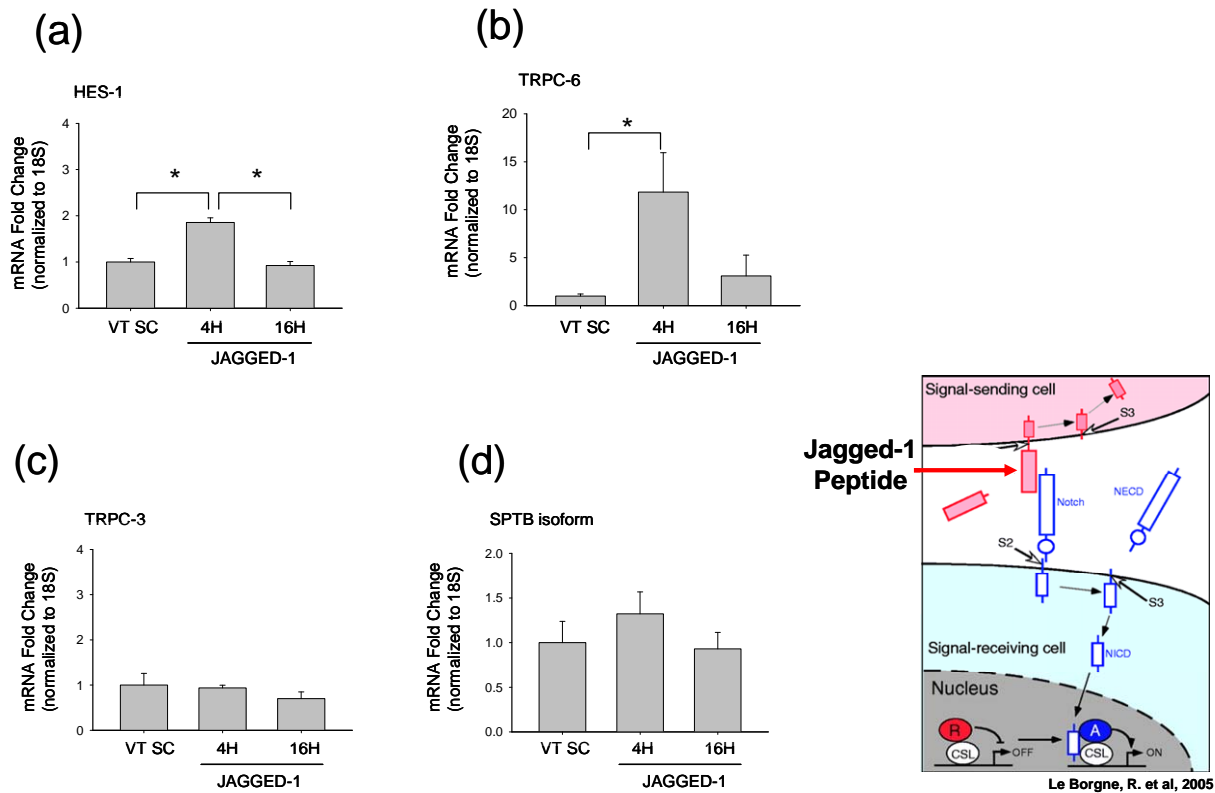


**Figure 18. Notch activation induces the expression of TRPC6 in PC12 cells**

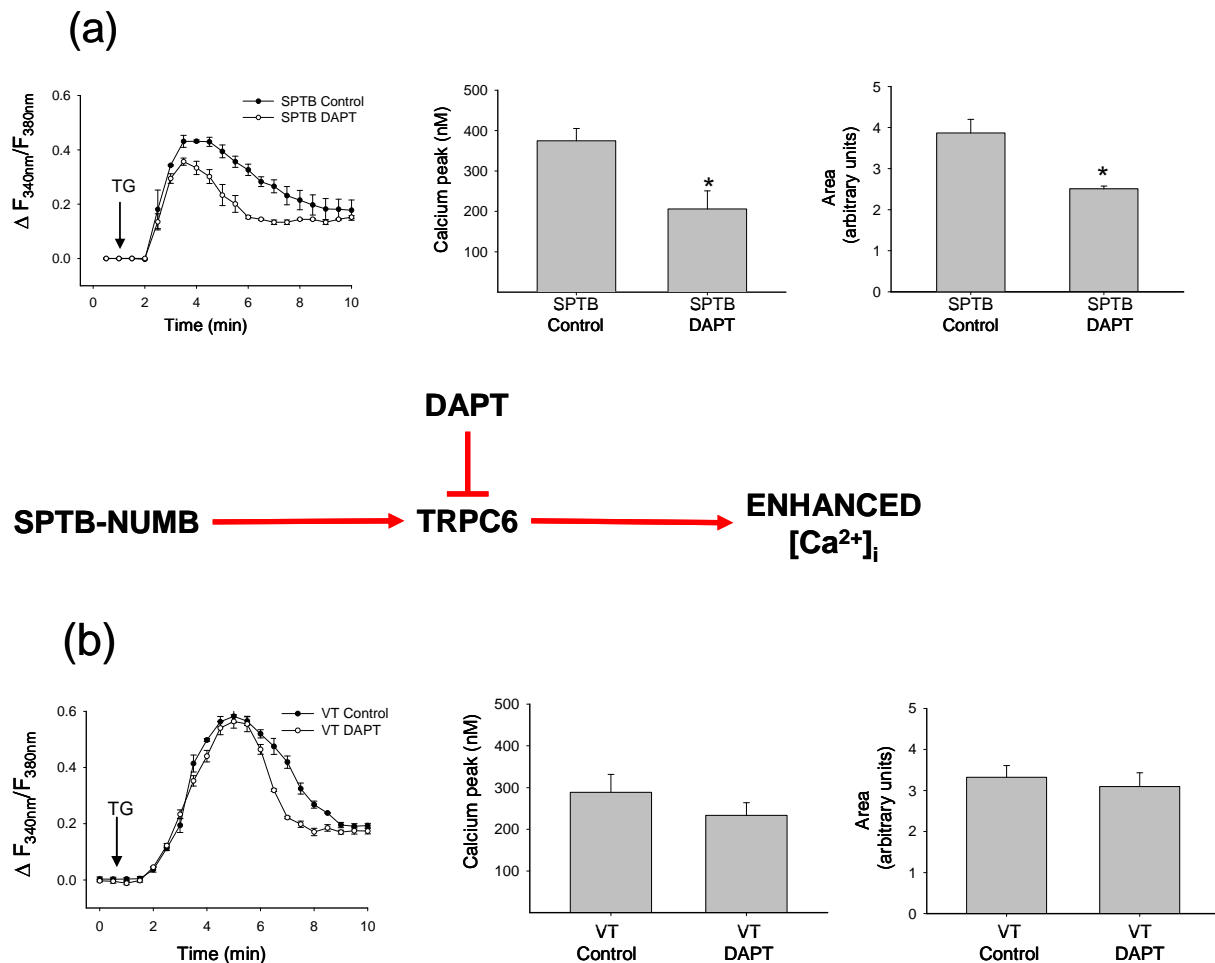
PC12 cells (VT) were treated with Jagged-1 peptide (15 $\mu$ M), or scramble control peptide (SC) (15 $\mu$ M) for designated times and the expression of various genes was assessed. Fold changes in mRNA of **(a)** HES-1 (n=4; \*p<0.001), **(b)** TRPC6 (n=4; \*p=0.015), **(c)** TRPC3 (n=4), and **(d)** SPTB isoform of Numb (n=4) after Jagged-1 treatment compared to scramble control (VT SC). Data are mean  $\pm$  SEM.

### ***Increased levels of TRPC6 channels account for the enhanced SOCE in SPTB-Numb***

We have shown that TRCP6 is upregulated in SPTB-Numb and that DAPT treatment attenuates its expression via a mechanism that involves Notch signaling. It is conceivable that the

increased levels of TRPC6 calcium channels may partly explain the increased ER calcium pool and enhanced SOCE in SPTB-Numb. Therefore, we tested whether DAPT treatment can reduce  $[Ca^{2+}]_i$  in response to thapsigargin treatment by attenuating TRPC6 expression. Changes in  $[Ca^{2+}]_i$  were assessed in vector and SPTB-Numb after treatment with thapsigargin calcium-free solution. The calcium response to thapsigargin treatment was reduced in SPTB-Numb pre-treated with DAPT for 24 h compared to untreated control (**Fig 19.a; left panel**). These differences in  $[Ca^{2+}]_i$  after thapsigargin-induced depletion of calcium pool were manifested by a reduced calcium peak ( $374.6 \pm 30.42$  vs.  $205.9 \pm 44.96$ ) (**Fig 19.a; center panel**), as well as by an overall attenuated calcium response to thapsigargin, assessed by calculating the area under the curve for each treatment ( $3.87 \pm 0.33$  vs.  $2.5 \pm 0.06$ ) (**Fig 19.a; right panel**). VT pre-treated with DAPT did not induce any changes in  $[Ca^{2+}]_i$  under similar conditions (**Fig 19.b**). Additionally, we tested whether DAPT treatment would also affect SOCE in VT and SPTB-Numb. Cells were treated with thapsigargin in calcium-free solution until steady state was reached. Calcium (2mM) was added in the medium and  $[Ca^{2+}]_i$  was recorded. Pre-treatment with DAPT for 24 h significantly decreased SOCE in SPTB-Numb (**Fig 19.c**), but not in VT (**Fig 19.d**). In order to exclude the possibility that these changes are mediated by an upregulation of proteins that are known to facilitate ER calcium uptake and sequestration, we assessed the protein levels of SERCA and Grp78/94 respectively. There were no differences in the protein levels of SERCA and Grp78/94 (**Fig 19.e**). Finally, in order to demonstrate the direct role of TRPC6 in enhancing SOCE in SPTB-Numb, we used siRNA to knock down TRPC6. The mRNA and protein levels of TRPC6 were significantly reduced ( $0.38 \pm 0.12$ -fold and  $0.47 \pm 0.02$ -fold respectively) compared to scramble (SC) control peptide (**Fig 19.f**). We set to confirm that the changes in  $[Ca^{2+}]_i$  upon DAPT pre-treatment and thapsigargin-induced calcium depletion specifically reflect calcium

influx via TRPC6 channels. We measured the effects of extracellular  $MnCl_2$  ( $Mn^{2+}$  200 $\mu$ M) on the rate at which Fura-2 fluorescence at 360nm ( $F_{360}$ ) was quenched.  $Mn^{2+}$  enters the cell as a  $Ca^{2+}$  surrogate and reduces  $F_{360}$  upon binding to the dye. The rate of quenched  $F_{360}$  was assessed in the presence of thapsigargin (ER  $Ca^{2+}$  store depletion) to measure  $Ca^{2+}$  influx in SPTB-Numb treated with either siTRPC6 or scramble control peptide. Quenching of  $F_{360}$  by  $Mn^{2+}$  was lower in siTRPC6 treated SPTB-Numb (shown on the trace are higher F/F0), suggesting that  $Ca^{2+}$  influx was significantly lower when TRPC6 was knocked down (**Fig 19.g**). Collectively, these results demonstrate that the TRPC6 upregulation may in part account for the enhanced SOCE that characterize the SPTB-Numb.



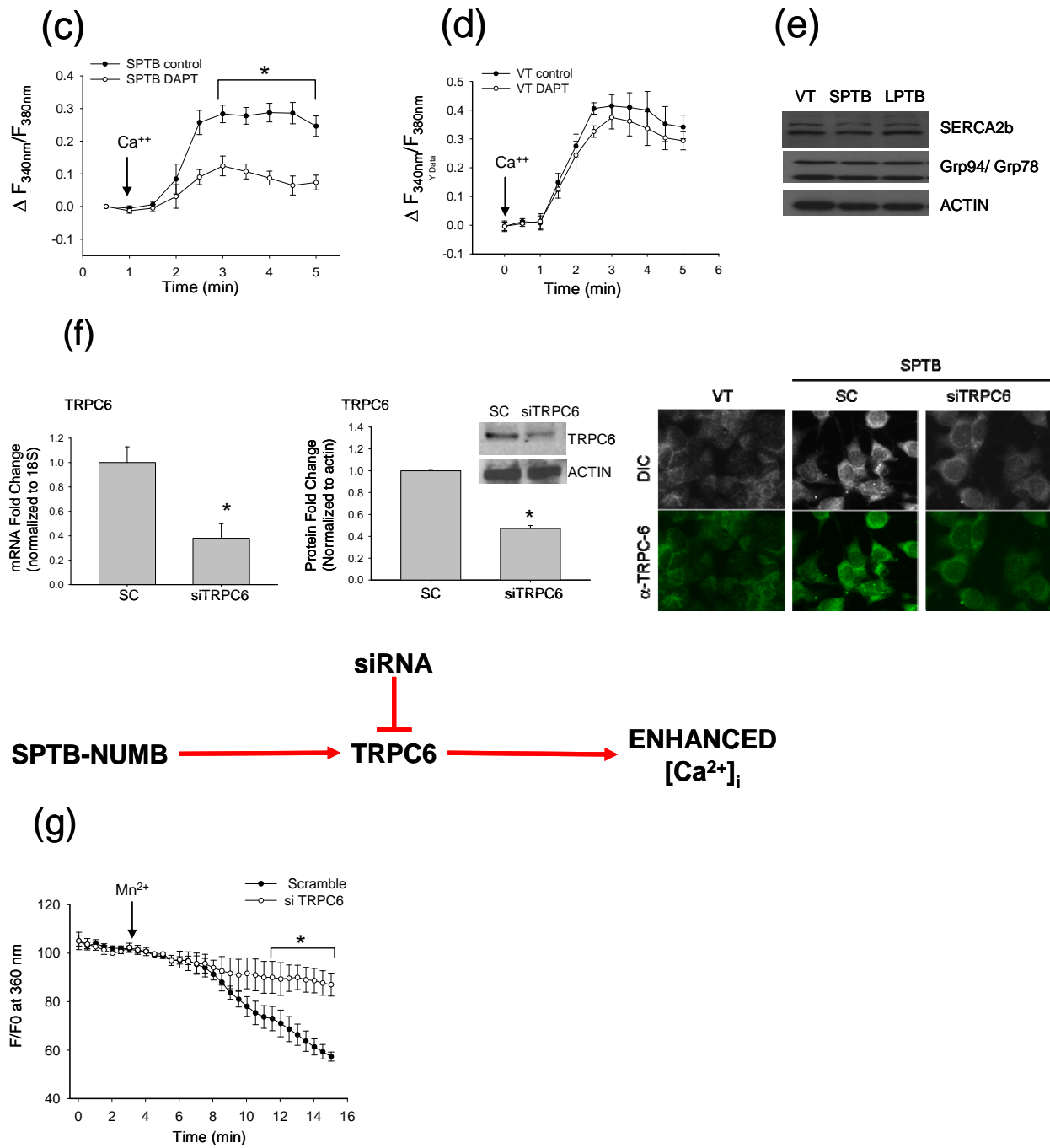


**Figure 19. TRPC6 upregulation mediates the enhanced SOCE in SPTB-Numb**

**(a)** SPTB-Numb were pre-treated with DAPT (40 $\mu$ M) in OptiMEM or OptiMEM alone for 24h. Cells were then perfused with Locke's Ca<sup>2+</sup>-free medium with 100 $\mu$ M EGTA for 6 minutes. Thapsigargin (1mM) was added, as indicated, and fluorescent ratio changes from baseline ( $\Delta F_{340}/F_{380}$ ) were recorded, in 30 second intervals, until steady state was reached (left panel). Ca<sup>2+</sup> peak was assessed as the largest change of [Ca<sup>2+</sup>]<sub>i</sub> from baseline (n=4; \*p=0.36) (center panel). The area under the curve was calculated as the sum of individual trapezoid areas (n=4; \*p<0.01) (right panel). **(b)** Same as described in (a) using VT (n=4). **(c)** SPTB-Numb were pretreated with DAPT (40 $\mu$ M) in OPTIMEM or OPTIMEM alone for 24h. Cells were then perfused with Locke's Ca<sup>2+</sup>-free medium with 100 $\mu$ M EGTA for 6 minutes and thapsigargin (1mM) was then added for 20 minutes. Cells were then perfused with Locke's including Ca<sup>2+</sup> (2mM), as indicated, and SOCE was recorded as fluorescent ratio changes from baseline ( $\Delta F_{340}/F_{380}$ ), in 30 second intervals (n=4; \*p<0.02) (left panel). **(d)** Same as described in (c) using VT (n=4). **(e)** Western blots showing protein levels of SERCA, Grp94/Grp78 and actin as loading control among VT, SPTB-Numb and LPTB-Numb. **(f)** Fold change of TRCP6 mRNA (n=6; \*p=0.01, left panel) and protein (n=3; \*p=0.004, center panel) levels of SPTB-Numb treated with TRPC6 siRNA (siTRPC6), or scramble (SC) control. Fluorescent intensity and localization of TRCP6 in SPTB-Numb treated with siTRPC6 compared to VT or scramble control (right panel). **(g)** Comparison of Mn<sup>2+</sup> quenching of Fura-2 fluorescence in SPTB-Numb treated with siTRPC6 or scramble control. Traces illustrate the time course and magnitude of Mn<sup>2+</sup> quenching. The fluorescence as a function of time (F) was normalized to the fluorescent value measured immediately before the addition of Mn<sup>2+</sup> (F0) (n=3; \*p<0.05 vs. scramble). Data are mean  $\pm$  SEM.



## *Discussion*

Mammalian Numb produce four isoforms that differ in the length of their PTB and/or PRR domains<sup>59, 65</sup>. In neural progenitor cells, Numb isoforms containing the long PRR domain promote proliferation, while those cells lacking the insert promote cell differentiation<sup>65</sup>. In NGF-induced differentiated PC12, Numb isoform lacking the insert at the PTB domain enhances neurite outgrowth compared to the isoforms containing the insert<sup>27</sup>. As such, it is conceivable that Numb may regulate diverse cell functions in an isoform specific way. We have previously shown that Numb modifies neural cell calcium homeostasis in an isoform-specific manner, and thereby may regulate cell survival<sup>26</sup>. More specifically, SPTB-Numb demonstrated increased calcium responses to bradykinin and enhanced  $[Ca^{2+}]_i$  after serum deprivation. These data suggest that Numb may mediate mechanisms that affect the ER calcium pool, thus regulating calcium-dependent processes.

Here we show that Numb affects SOCE in an isoform-specific manner via a mechanism that induces transcriptional upregulation of TRPC calcium channels. TRPC belong to the superfamily of TRP calcium channels that are activated in response to receptor stimulation and activation of different isoforms of protein lipase C (PLC), or activation by diacylglycerol (DAG)<sup>73, 129, 130</sup>. Despite the unequivocal role of TRPC in receptor-mediated calcium entry, their involvement in SOCE has not been well characterized<sup>131, 132</sup>. In neuroblasts, serum deprivation induces ER store depletion, a process that activates SOCE mechanisms<sup>133</sup>. Therefore, we tested whether the TRPC calcium channels are involved in the serum deprivation-induced susceptibility to cell death in neural cells. Serum deprivation selectively upregulated TRPC6 channels in PC12 cells, consistent with a recent report where chronic hypoxia in pulmonary arterial smooth muscle

cells increased TRPC6 leading to enhanced  $\text{Ca}^{2+}$  entry through SOCE mechanisms <sup>76</sup>. We also found that TRPC6 accumulated at the plasma membrane of PC12 consistent with reports showing that SOC channels transported in cytoplasmic vesicles fuse with the plasma membrane to mediate SOCE <sup>134, 135</sup>. Furthermore, siRNA against TRPC6 significantly protected PC12 cells from serum deprivation confirming the selective role of TRPC6 in mediating serum deprivation-induced cell death by altering calcium homeostasis. Accordingly, siTRPC6 reduced calcium influx in SPTB-Numb after calcium store depletion demonstrating that high levels of TRPC6 can mediate SOCE mechanisms. Consistent with our findings, TRPC6 channels translocated to the plasma membrane in response to store depletion by thapsigargin, indicating a store-dependent involvement of TRPC6 channels <sup>136</sup>. TRPC6 can be directly activated by receptor-operated signaling resulting in activated PLC or increased DAG, without the involvement of internal calcium stores <sup>73</sup>. Our results however, suggest that TRPC6 is involved in SOCE, induced by depletion of ER calcium pool. TRPC6 and TRPC3 are largely non-selective cation channels, suggesting that the inward current passing through them can be attributed to  $\text{Na}^+$  ions <sup>137, 138</sup>. Along these lines, stimulation of  $\text{Ca}^{2+}$  entry via TRPC6 channels in A7r5 smooth muscle cells was abolished by voltage-gated calcium channel blockers, suggesting that  $\text{Na}^+$  entry through TRPC6 and the subsequent membrane depolarization induced much of  $\text{Ca}^{2+}$  influx <sup>139</sup>. The expression levels of TRPC6 and TRPC3 in SPTB-Numb was approximately 100-fold and 36-fold higher respectively compared to VT. Moreover, the SPTB-Numb display phenotypic characteristic similar to differentiated PC12 cells <sup>27</sup>, which express high levels of L-type  $\text{Ca}^{2+}$  channels <sup>140</sup>. Conceivably, it is possible that the involvement of TRPC6 in SOCE is mediated by secondary effects on membrane depolarization and activation of L-type  $\text{Ca}^{2+}$  channels.

During embryogenesis, Numb antagonizes the functions of Notch; however, Numb is expressed in many adult mammalian cells suggesting additional functions that may also be mediated by Notch. The biochemical mechanism by which Numb antagonizes Notch is not clear<sup>56, 122, 141, 142</sup>. It has been suggested that Numb interacts with NICD preventing its nuclear localization and therefore transcriptional activity<sup>143</sup>. More specifically, Numb induces ubiquitination of Notch1 by recruiting the E3 ligase Itch, a process that requires the PTB domain of Numb<sup>58</sup>. These data suggest that the Numb isoforms that differ in the PTB domain may differentially regulate Notch activity. Indeed, we found increased levels of NICD in SPTB-Numb compared to VT and LPTB-Numb. NICD was primarily localized to nucleus of SPTB-Numb resulting in increased expression of HES-1, a known transcriptional target to Notch signaling. Therefore, it is possible that Notch may mediate the transcriptional upregulation of TRCP6 in SPTB-Numb. We used DAPT, a known  $\gamma$ -secretase inhibitor, to reduce the release of NICD, thereby attenuating Notch activity. Consistent with our hypothesis, DAPT reduced the expression of TRPC6 in SPTB-Numb. Furthermore, activation of Notch by jagged-1 peptide, a known Notch ligand, induced increases in TRPC6 expression in VT, confirming that Notch mediates the transcriptional upregulation of TRPC6 in SPTB-Numb. DAPT treatment in SPTB-Numb also reduced ER calcium pool and attenuated  $[Ca^{2+}]_i$  in response to store depletion consistent with the changes in TRPC6 expression.

Notch signaling plays an important role in cell differentiation, proliferation and apoptosis<sup>144</sup>, therefore we tested whether serum deprivation would enhance Notch activity in neural cells illuminating its role on TRPC6 transcriptional regulation. Serum deprivation increased the levels of NICD in neural cells and induced its nuclear translocation in a time-dependent manner consistent with the observed increases in the TRPC6 levels. Our results are in accordance with

previous findings where NICD levels were significantly elevated after cerebral ischemia in mice, while intravenous infusion of DAPT reduced NICD levels and ameliorated ischemia-induced brain damage<sup>145</sup>.

Interestingly, the changes in Notch activity and the concomitant upregulation in TRPC6 were preceded by a significant switch in Numb isoform expression favoring the upregulation of the SPTB over the LPTB Numb isoform. This early upregulation of SPTB Numb isoform after serum deprivation supports the notion that Numb may modulate Notch activity in an isoform specific manner. Interestingly, LPTB-Numb suppressed serum deprivation-induced activation of Notch and the subsequent upregulation of TRPC6 and conferred protection against cell death. The latter finding further strengthens the link between the Numb isoform specific effect on Notch activation and the Notch-dependent upregulation of TRPC6. Numb colocalized with endocytic vesicles and was shown to directly bind to Notch as well as the ear domain of  $\alpha$ -adaptin<sup>115</sup>. These findings dictate a role of Numb as an adaptor between  $\alpha$ -adaptin and Notch promoting the down-regulation of Notch by endocytosis. We have shown that the PTB Numb isoforms differentially affect the sorting of APP to the recycling and degradative pathways (Kyriazis GA, et al., 2008). Accordingly, in SPTB-Numb Notch was found to accumulate in the early endosome where it was shown to colocalize with Rab5a, an early endosomal marker. It has been suggested that endocytosis is important in NICD release and signaling. For instance, inhibition of the late endosome can activate Notch signaling by redirecting its trafficking via the early endosomal compartments<sup>146</sup>. Therefore, accumulation of Notch in early endocytic compartments may lead to its activation suggesting that  $\gamma$ -secretase activity occurs in places other than the cell surface<sup>147</sup>. It is possible that the SPTB Numb isoform induces ectopic

activation of Notch by directing its sorting in compartments where  $\gamma$ -secretase-mediated proteolytic processing is present.

In summary, we showed that Numb can modulate calcium homeostasis in an isoform-specific manner by increasing the transcription of TRCP6 calcium channels. These effects of Numb are mediated by an isoform-specific regulation of Notch activity. Moreover, serum deprivation induces Notch activation and TRPC6 upregulation resulting in calcium dysregulation and cell death (**Fig 20**). The consequences of Notch-mediated TRPC6 regulation in disease models are not known yet. Notch signaling is activated upon ischemic stroke suggesting a contribution of Notch to neuronal cell death<sup>145</sup>. It is plausible that during stress Notch mediates its detrimental effects by specifically targeting TRPC6 and calcium homeostasis. Although, this is the first report showing that TRCP6 is a transcriptional target of Notch signaling, the precise transcriptional mechanism remains known. Finally, understanding the factors that regulate the alternative splicing of Numb proteins may serve as a molecular target to control the functions of Notch and its downstream signals.

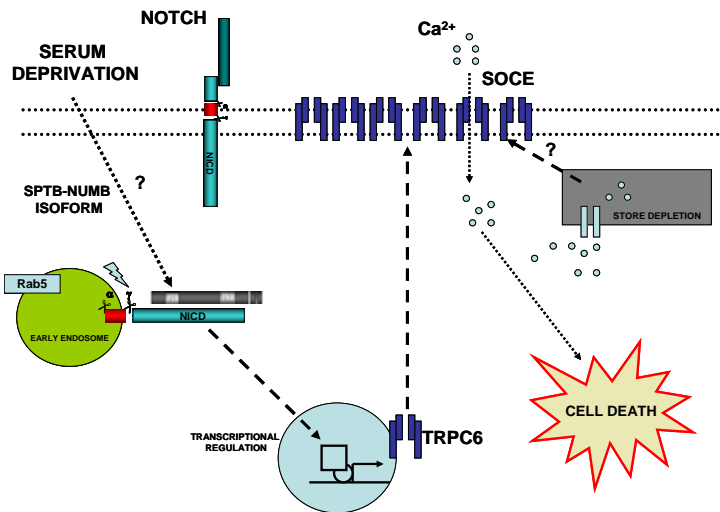


**Figure 20. Schematic diagram: SPTB-Numb affect the Notch-dependent upregulation of TRPC6 calcium channels**

In pro-neuronal PC12 cells, serum deprivation selectively upregulates the SPTB isoform of numb, favoring the shorting of Notch at early endosomal compartments, inducing an increase in NICD generation and Notch transcriptional activity. In turn, Notch mediates the transcriptional upregulation of TRPC6 calcium channels, which regulate calcium homeostasis via a store-operated calcium entry (SOCE) mechanism. The notch-mediated TRPC6 upregulation and its subsequent effects on calcium flux partly account for the serum deprivation-induced cell death in PC12 cells.

## REFERENCES

1. Mattson, M.P. Cellular actions of beta-amyloid precursor protein and its soluble and fibrillogenic derivatives. *Physiol Rev.* **77**, 1081-1132 (1997).
2. Gandy, S., Caporaso, G., Buxbaum, J., Frangione, B., & Greengard, P. APP processing, A beta-amyloidogenesis, and the pathogenesis of Alzheimer's disease. *Neurobiol. Aging* **15**, 253-256 (1994).
3. Selkoe, D.J. Alzheimer's disease: genes, proteins, and therapy. *Physiol Rev.* **81**, 741-766 (2001).
4. Selkoe, D.J. *et al.* The role of APP processing and trafficking pathways in the formation of amyloid beta-protein. *Ann. N. Y. Acad. Sci.* **777**, 57-64 (1996).
5. Weidemann, A. *et al.* Identification, biogenesis, and localization of precursors of Alzheimer's disease A4 amyloid protein. *Cell* **57**, 115-126 (1989).
6. Haass, C., Koo, E.H., Mellon, A., Hung, A.Y., & Selkoe, D.J. Targeting of cell-surface beta-amyloid precursor protein to lysosomes: alternative processing into amyloid-bearing fragments. *Nature* **357**, 500-503 (1992).
7. Carey, R.M., Balcz, B.A., Lopez-Coviella, I., & Slack, B.E. Inhibition of dynamin-dependent endocytosis increases shedding of the amyloid precursor protein ectodomain and reduces generation of amyloid beta protein. *BMC. Cell Biol.* **6**, 30 (2005).
8. Koo, E.H. & Squazzo, S.L. Evidence that production and release of amyloid beta-protein involves the endocytic pathway. *J Biol. Chem.* **269**, 17386-17389 (1994).
9. Uemura, T., Shepherd, S., Ackerman, L., Jan, L.Y., & Jan, Y.N. numb, a gene required in determination of cell fate during sensory organ formation in Drosophila embryos. *Cell* **58**, 349-360 (1989).
10. Rhyu, M.S., Jan, L.Y., & Jan, Y.N. Asymmetric distribution of numb protein during division of the sensory organ precursor cell confers distinct fates to daughter cells. *Cell* **76**, 477-491 (1994).
11. Dho, S.E., French, M.B., Woods, S.A., & McGlade, C.J. Characterization of four mammalian numb protein isoforms. Identification of cytoplasmic and membrane-associated variants of the phosphotyrosine binding domain. *J Biol. Chem.* **274**, 33097-33104 (1999).
12. Verdi, J.M. *et al.* Mammalian NUMB is an evolutionarily conserved signaling adapter protein that specifies cell fate. *Curr. Biol.* **6**, 1134-1145 (1996).

13. Berdnik,D., Torok,T., Gonzalez-Gaitan,M., & Knoblich,J.A. The endocytic protein alpha-Adaptin is required for numb-mediated asymmetric cell division in *Drosophila*. *Dev. Cell* **3**, 221-231 (2002).
14. Santolini,E. *et al.* Numb is an endocytic protein. *J Cell Biol.* **151**, 1345-1352 (2000).
15. Guo,M., Jan,L.Y., & Jan,Y.N. Control of daughter cell fates during asymmetric division: interaction of Numb and Notch. *Neuron* **17**, 27-41 (1996).
16. Huang,E.J. *et al.* Targeted deletion of numb and numbl like in sensory neurons reveals their essential functions in axon arborization. *Genes Dev.* **19**, 138-151 (2005).
17. Wakamatsu,Y., Maynard,T.M., Jones,S.U., & Weston,J.A. NUMB localizes in the basal cortex of mitotic avian neuroepithelial cells and modulates neuronal differentiation by binding to NOTCH-1. *Neuron* **23**, 71-81 (1999).
18. Mumm,J.S. & Kopan,R. Notch signaling: from the outside in. *Dev. Biol.* **228**, 151-165 (2000).
19. McGill,M.A. & McGlade,C.J. Mammalian numb proteins promote Notch1 receptor ubiquitination and degradation of the Notch1 intracellular domain. *J Biol. Chem.* **278**, 23196-23203 (2003).
20. Frise,E., Knoblich,J.A., Younger-Shepherd,S., Jan,L.Y., & Jan,Y.N. The *Drosophila* Numb protein inhibits signaling of the Notch receptor during cell-cell interaction in sensory organ lineage. *Proc. Natl. Acad. Sci. U. S. A* **93**, 11925-11932 (1996).
21. Spana,E.P. & Doe,C.Q. Numb antagonizes Notch signaling to specify sibling neuron cell fates. *Neuron* **17**, 21-26 (1996).
22. Nishimura,T. *et al.* CRMP-2 regulates polarized Numb-mediated endocytosis for axon growth. *Nat. Cell Biol.* **5**, 819-826 (2003).
23. Nishimura,T. & Kaibuchi,K. Numb controls integrin endocytosis for directional cell migration with aPKC and PAR-3. *Dev. Cell* **13**, 15-28 (2007).
24. Roncarati,R. *et al.* The gamma-secretase-generated intracellular domain of beta-amyloid precursor protein binds Numb and inhibits Notch signaling. *Proc. Natl. Acad. Sci. U. S. A* **99**, 7102-7107 (2002).
25. King,G.D. & Scott,T.R. Adaptor protein interactions: modulators of amyloid precursor protein metabolism and Alzheimer's disease risk? *Exp. Neurol.* **185**, 208-219 (2004).



26. Chan,S.L., Pedersen,W.A., Zhu,H., & Mattson,M.P. Numb modifies neuronal vulnerability to amyloid beta-peptide in an isoform-specific manner by a mechanism involving altered calcium homeostasis: implications for neuronal death in Alzheimer's disease. *Neuromolecular. Med.* **1**, 55-67 (2002).
27. Pedersen,W.A. *et al.* Numb isoforms containing a short PTB domain promote neurotrophic factor-induced differentiation and neurotrophic factor withdrawal-induced death of PC12 Cells. *J. Neurochem.* **82**, 976-986 (2002).
28. Rebel,V.I. *et al.* One-day ex vivo culture allows effective gene transfer into human nonobese diabetic/severe combined immune-deficient repopulating cells using high-titer vesicular stomatitis virus G protein pseudotyped retrovirus. *Blood* **93**, 2217-2224 (1999).
29. Sever,S., Damke,H., & Schmid,S.L. Dynamin:GTP controls the formation of constricted coated pits, the rate limiting step in clathrin-mediated endocytosis. *J. Cell Biol.* **150**, 1137-1148 (2000).
30. Ikin,A.F. *et al.* Alzheimer amyloid protein precursor is localized in nerve terminal preparations to Rab5-containing vesicular organelles distinct from those implicated in the synaptic vesicle pathway. *J. Biol. Chem.* **271**, 31783-31786 (1996).
31. Ferreira,A., Caceres,A., & Kosik,K.S. Intraneuronal compartments of the amyloid precursor protein. *J. Neurosci.* **13**, 3112-3123 (1993).
32. Fenteany,G. *et al.* Inhibition of proteasome activities and subunit-specific amino-terminal threonine modification by lactacystin. *Science* **268**, 726-731 (1995).
33. Lai,E.C. Notch cleavage: Nicastrin helps Presenilin make the final cut. *Curr. Biol.* **12**, R200-R202 (2002).
34. Caporaso,G.L. *et al.* Morphologic and biochemical analysis of the intracellular trafficking of the Alzheimer beta/A4 amyloid precursor protein. *J. Neurosci.* **14**, 3122-3138 (1994).
35. Beers,M.F. Inhibition of cellular processing of surfactant protein C by drugs affecting intracellular pH gradients. *J. Biol. Chem.* **271**, 14361-14370 (1996).
36. Stein,B.S., Bensch,K.G., & Sussman,H.H. Complete inhibition of transferrin recycling by monensin in K562 cells. *J. Biol. Chem.* **259**, 14762-14772 (1984).
37. Verdi,J.M. *et al.* Distinct human NUMB isoforms regulate differentiation vs. proliferation in the neuronal lineage. *Proc. Natl. Acad. Sci. U. S. A* **96**, 10472-10476 (1999).
38. Bani-Yaghub,M. *et al.* A switch in numb isoforms is a critical step in cortical development. *Dev. Dyn.* **236**, 696-705 (2007).

39. Juven-Gershon, T. *et al.* The Mdm2 oncoprotein interacts with the cell fate regulator Numb. *Mol. Cell Biol.* **18**, 3974-3982 (1998).
40. Susini, L. *et al.* Siah-1 binds and regulates the function of Numb. *Proc. Natl. Acad. Sci. U. S. A* **98**, 15067-15072 (2001).
41. Zhou, M.M. *et al.* Structure and ligand recognition of the phosphotyrosine binding domain of Shc. *Nature* **378**, 584-592 (1995).
42. Li, S.C. *et al.* Structure of a Numb PTB domain-peptide complex suggests a basis for diverse binding specificity. *Nat. Struct. Biol.* **5**, 1075-1083 (1998).
43. Yaich, L. *et al.* Functional analysis of the Numb phosphotyrosine-binding domain using site-directed mutagenesis. *J. Biol. Chem.* **273**, 10381-10388 (1998).
44. Zwahlen, C., Li, S.C., Kay, L.E., Pawson, T., & Forman-Kay, J.D. Multiple modes of peptide recognition by the PTB domain of the cell fate determinant Numb. *EMBO J.* **19**, 1505-1515 (2000).
45. Dho, S.E. *et al.* The mammalian numb phosphotyrosine-binding domain. Characterization of binding specificity and identification of a novel PDZ domain-containing numb binding protein, LNX. *J. Biol. Chem.* **273**, 9179-9187 (1998).
46. Di, M.L. *et al.* Numb is a suppressor of Hedgehog signalling and targets Gli1 for Itch-dependent ubiquitination. *Nat. Cell Biol.* **8**, 1415-1423 (2006).
47. Cataldo, A.M., Barnett, J.L., Pieroni, C., & Nixon, R.A. Increased neuronal endocytosis and protease delivery to early endosomes in sporadic Alzheimer's disease: neuropathologic evidence for a mechanism of increased beta-amyloidogenesis. *J. Neurosci.* **17**, 6142-6151 (1997).
48. Grbovic, O.M. *et al.* Rab5-stimulated up-regulation of the endocytic pathway increases intracellular beta-cleaved amyloid precursor protein carboxyl-terminal fragment levels and A $\beta$  production. *J Biol. Chem.* **278**, 31261-31268 (2003).
49. Smith, C.A., Dho, S.E., Donaldson, J., Tepass, U., & McGlade, C.J. The cell fate determinant numb interacts with EHD/Rme-1 family proteins and has a role in endocytic recycling. *Mol. Biol. Cell* **15**, 3698-3708 (2004).
50. Souza-Schorey, C., Li, G., Colombo, M.I., & Stahl, P.D. A regulatory role for ARF6 in receptor-mediated endocytosis. *Science* **267**, 1175-1178 (1995).
51. Verbeek, M.M., Otte-Holler, I., Fransen, J.A., & de Waal, R.M. Accumulation of the amyloid-beta precursor protein in multivesicular body-like organelles. *J. Histochem. Cytochem.* **50**, 681-690 (2002).

52. Mattson, M.P. & Chan, S.L. Dysregulation of cellular calcium homeostasis in Alzheimer's disease: bad genes and bad habits. *J. Mol. Neurosci.* **17**, 205-224 (2001).
53. Jan, Y.N. & Jan, L.Y. Asymmetric cell division. *Nature* **392**, 775-778 (1998).
54. Zhong, W. *et al.* Mouse numb is an essential gene involved in cortical neurogenesis. *Proc. Natl. Acad. Sci. U. S. A* **97**, 6844-6849 (2000).
55. Bray, S. A Notch affair. *Cell* **93**, 499-503 (1998).
56. Spana, E.P. & Doe, C.Q. Numb antagonizes Notch signaling to specify sibling neuron cell fates. *Neuron* **17**, 21-26 (1996).
57. Zhong, W., Feder, J.N., Jiang, M.M., Jan, L.Y., & Jan, Y.N. Asymmetric localization of a mammalian numb homolog during mouse cortical neurogenesis. *Neuron* **17**, 43-53 (1996).
58. McGill, M.A. & McGlade, C.J. Mammalian numb proteins promote Notch1 receptor ubiquitination and degradation of the Notch1 intracellular domain. *J. Biol. Chem.* **278**, 23196-23203 (2003).
59. Dho, S.E., French, M.B., Woods, S.A., & McGlade, C.J. Characterization of four mammalian numb protein isoforms. Identification of cytoplasmic and membrane-associated variants of the phosphotyrosine binding domain. *J. Biol. Chem.* **274**, 33097-33104 (1999).
60. Verdi, J.M. *et al.* Mammalian NUMB is an evolutionarily conserved signaling adapter protein that specifies cell fate. *Curr. Biol.* **6**, 1134-1145 (1996).
61. Zhong, W., Jiang, M.M., Weinmaster, G., Jan, L.Y., & Jan, Y.N. Differential expression of mammalian Numb, Numlike and Notch1 suggests distinct roles during mouse cortical neurogenesis. *Development* **124**, 1887-1897 (1997).
62. Zilian, O. *et al.* Multiple roles of mouse Numb in tuning developmental cell fates. *Curr. Biol.* **11**, 494-501 (2001).
63. Bork, P. & Margolis, B. A phosphotyrosine interaction domain. *Cell* **80**, 693-694 (1995).
64. Salcini, A.E. *et al.* Binding specificity and in vivo targets of the EH domain, a novel protein-protein interaction module. *Genes Dev.* **11**, 2239-2249 (1997).
65. Verdi, J.M. *et al.* Distinct human NUMB isoforms regulate differentiation vs. proliferation in the neuronal lineage. *Proc. Natl. Acad. Sci. U. S. A* **96**, 10472-10476 (1999).

66. Berridge, M.J., Lipp, P., & Bootman, M.D. The versatility and universality of calcium signalling. *Nat. Rev. Mol. Cell Biol.* **1**, 11-21 (2000).
67. Friel, D.D. & Chiel, H.J. Calcium dynamics: analyzing the Ca<sup>2+</sup> regulatory network in intact cells. *Trends in Neurosciences* **31**, 8-19 (2008).
68. Berridge, M.J., Lipp, P., & Bootman, M.D. Signal transduction. The calcium entry pas de deux. *Science* **287**, 1604-1605 (2000).
69. Mattson, M.P. Calcium and neurodegeneration. *Aging Cell* **6**, 337-350 (2007).
70. Janssen, L.J. & Kwan, C.Y. ROCs and SOCs: What's in a name? *Cell Calcium* **41**, 245-247 (2007).
71. Pedersen, S.F., Owsianik, G., & Nilius, B. TRP channels: an overview. *Cell Calcium* **38**, 233-252 (2005).
72. Soboloff, J. *et al.* TRPC channels: integrators of multiple cellular signals. *Handb. Exp. Pharmacol.* 575-591 (2007).
73. Hofmann, T. *et al.* Direct activation of human TRPC6 and TRPC3 channels by diacylglycerol. *Nature* **397**, 259-263 (1999).
74. Hoth, M. & Penner, R. Depletion of intracellular calcium stores activates a calcium current in mast cells. *Nature* **355**, 353-356 (1992).
75. Parekh, A.B. & Penner, R. Store depletion and calcium influx. *Physiol Rev.* **77**, 901-930 (1997).
76. Wang, J. *et al.* Hypoxia inducible factor 1 mediates hypoxia-induced TRPC expression and elevated intracellular Ca<sup>2+</sup> in pulmonary arterial smooth muscle cells. *Circ. Res.* **98**, 1528-1537 (2006).
77. Cayouette, S., Lussier, M.P., Mathieu, E.L., Bousquet, S.M., & Boulay, G. Exocytotic insertion of TRPC6 channel into the plasma membrane upon Gq protein-coupled receptor activation. *J. Biol. Chem.* **279**, 7241-7246 (2004).
78. Hofmann, T., Schaefer, M., Schultz, G., & Gudermann, T. Subunit composition of mammalian transient receptor potential channels in living cells. *Proc. Natl. Acad. Sci. U. S. A* **99**, 7461-7466 (2002).
79. Kim, J.Y. & Saffen, D. Activation of M1 muscarinic acetylcholine receptors stimulates the formation of a multiprotein complex centered on TRPC6 channels. *J. Biol. Chem.* **280**, 32035-32047 (2005).
80. Reiser, J. *et al.* TRPC6 is a glomerular slit diaphragm-associated channel required for normal renal function. *Nat. Genet.* **37**, 739-744 (2005).

81. Winn,M.P. *et al.* A mutation in the TRPC6 cation channel causes familial focal segmental glomerulosclerosis. *Science* **308**, 1801-1804 (2005).
82. Wang,J., Shimoda,L.A., & Sylvester,J.T. Capacitative calcium entry and TRPC channel proteins are expressed in rat distal pulmonary arterial smooth muscle. *Am. J. Physiol Lung Cell Mol. Physiol* **286**, L848-L858 (2004).
83. Yu,Y. *et al.* Enhanced expression of transient receptor potential channels in idiopathic pulmonary arterial hypertension. *Proc. Natl. Acad. Sci. U. S. A* **101**, 13861-13866 (2004).
84. Onohara,N. *et al.* TRPC3 and TRPC6 are essential for angiotensin II-induced cardiac hypertrophy. *EMBO J.* **25**, 5305-5316 (2006).
85. Vandebrouck,C., Martin,D., Colson-Van,S.M., Debaix,H., & Gailly,P. Involvement of TRPC in the abnormal calcium influx observed in dystrophic (mdx) mouse skeletal muscle fibers. *J. Cell Biol.* **158**, 1089-1096 (2002).
86. Lessard,C.B., Lussier,M.P., Cayouette,S., Bourque,G., & Boulay,G. The overexpression of presenilin2 and Alzheimer's-disease-linked presenilin2 variants influences TRPC6-enhanced Ca<sup>2+</sup> entry into HEK293 cells. *Cell Signal.* **17**, 437-445 (2005).
87. Gordon,W.R. *et al.* Structural basis for autoinhibition of Notch. *Nat Struct Mol Biol* **14**, 295-300 (2007).
88. Logeat,F. *et al.* The Notch1 receptor is cleaved constitutively by a furin-like convertase. *Proceedings of the National Academy of Sciences* **95**, 8108-8112 (1998).
89. Nichols,J.T. *et al.* DSL ligand endocytosis physically dissociates Notch1 heterodimers before activating proteolysis can occur. *J. Cell Biol.* **176**, 445-458 (2007).
90. Rand,M.D. *et al.* Calcium depletion dissociates and activates heterodimeric notch receptors. *Mol Cell Biol* **20**, 1825-1835 (2000).
91. Fehon,R.G. *et al.* Molecular interactions between the protein products of the neurogenic loci Notch and Delta, two EGF-homologous genes in *Drosophila*. *Cell* **61**, 523-534 (1990).
92. Lissemore,J.L. & Starmer,W.T. Phylogenetic analysis of vertebrate and invertebrate Delta/Serrate/LAG-2 (DSL) proteins. *Mol Phylogenet. Evol.* **11**, 308-319 (1999).
93. Maine,E.M., Lissemore,J.L., & Starmer,W.T. A phylogenetic analysis of vertebrate and invertebrate Notch-related genes. *Mol Phylogenet. Evol.* **4**, 139-149 (1995).

94. Brou,C. *et al.* A novel proteolytic cleavage involved in Notch signaling: the role of the disintegrin-metalloprotease TACE. *Mol Cell* **5**, 207-216 (2000).
95. Lieber,T., Kidd,S., & Young,M.W. kuzbanian-mediated cleavage of Drosophila Notch. *Genes Dev.* **16**, 209-221 (2002).
96. Mumm,J.S. *et al.* A ligand-induced extracellular cleavage regulates gamma-secretase-like proteolytic activation of Notch1. *Mol Cell* **5**, 197-206 (2000).
97. Kopan,R., Schroeter,E.H., Weintraub,H., & Nye,J.S. Signal transduction by activated mNotch: importance of proteolytic processing and its regulation by the extracellular domain. *Proc. Natl. Acad. Sci. U. S. A* **93**, 1683-1688 (1996).
98. Schroeter,E.H., Kisslinger,J.A., & Kopan,R. Notch-1 signalling requires ligand-induced proteolytic release of intracellular domain. *Nature* **393**, 382-386 (1998).
99. Struhl,G. & Adachi,A. Nuclear access and action of notch in vivo. *Cell* **93**, 649-660 (1998).
100. Wolfe,M.S. The  $\gamma$ -Secretase Complex: Membrane-Embedded Proteolytic Ensemble. *Biochemistry* **45**, 7931-7939 (2006).
101. Fortini,M.E. & Artavanis-Tsakonas,S. The suppressor of hairless protein participates in notch receptor signaling. *Cell* **79**, 273-282 (1994).
102. Miele,L. & Osborne,B. Arbiter of differentiation and death: Notch signaling meets apoptosis. *J. Cell Physiol* **181**, 393-409 (1999).
103. Artavanis-Tsakonas,S., Rand,M.D., & Lake,R.J. Notch signaling: cell fate control and signal integration in development. *Science* **284**, 770-776 (1999).
104. Conlon,R.A., Reaume,A.G., & Rossant,J. Notch1 is required for the coordinate segmentation of somites. *Development* **121**, 1533-1545 (1995).
105. de la Pompa,J.L. *et al.* Conservation of the Notch signalling pathway in mammalian neurogenesis. *Development* **124**, 1139-1148 (1997).
106. Dunwoodie,S.L. *et al.* Axial skeletal defects caused by mutation in the spondylocostal dysplasia/pudgy gene Dll3 are associated with disruption of the segmentation clock within the presomitic mesoderm. *Development* **129**, 1795-1806 (2002).
107. Hamada,Y. *et al.* Mutation in ankyrin repeats of the mouse Notch2 gene induces early embryonic lethality. *Development* **126**, 3415-3424 (1999).
108. Hrabe de,A.M., McIntyre,J., & Gossler,A. Maintenance of somite borders in mice requires the Delta homologue Dll1. *Nature* **386**, 717-721 (1997).

109. Jiang,R. *et al.* Defects in limb, craniofacial, and thymic development in Jagged2 mutant mice. *Genes Dev.* **12**, 1046-1057 (1998).
110. Kusumi,K. *et al.* The mouse pudgy mutation disrupts Delta homologue Dll3 and initiation of early somite boundaries. *Nat Genet.* **19**, 274-278 (1998).
111. McCright,B. *et al.* Defects in development of the kidney, heart and eye vasculature in mice homozygous for a hypomorphic Notch2 mutation. *Development* **128**, 491-502 (2001).
112. Swiatek,P.J., Lindsell,C.E., del Amo,F.F., Weinmaster,G., & Gridley,T. Notch1 is essential for postimplantation development in mice. *Genes Dev.* **8**, 707-719 (1994).
113. Xue,Y. *et al.* Embryonic lethality and vascular defects in mice lacking the Notch ligand Jagged1. *Hum. Mol Genet.* **8**, 723-730 (1999).
114. Le,B.R., Bardin,A., & Schweisguth,F. The roles of receptor and ligand endocytosis in regulating Notch signaling. *Development* **132**, 1751-1762 (2005).
115. Berdnik,D., Torok,T., Gonzalez-Gaitan,M., & Knoblich,J.A. The endocytic protein alpha-Adaptin is required for numb-mediated asymmetric cell division in *Drosophila*. *Dev. Cell* **3**, 221-231 (2002).
116. Grynkiewicz,G., Poenie,M., & Tsien,R.Y. A new generation of Ca<sup>2+</sup> indicators with greatly improved fluorescence properties. *J. Biol Chem.* **260**, 3440-3450 (1985).
117. Livak,K.J. & Schmittgen,T.D. Analysis of relative gene expression data using real-time quantitative PCR and the 2<sup>-</sup>(Delta Delta C(T)) Method. *Methods* **25**, 402-408 (2001).
118. Neuhaus,R., Reber,B.F., & Reuter,H. Regulation of bradykinin- and ATP-activated Ca(2+)-permeable channels in rat pheochromocytoma (PC12) cells. *J. Neurosci.* **11**, 3984-3990 (1991).
119. Thastrup,O., Cullen,P.J., Drobak,B.K., Hanley,M.R., & Dawson,A.P. Thapsigargin, a tumor promoter, discharges intracellular Ca<sup>2+</sup> stores by specific inhibition of the endoplasmic reticulum Ca<sup>2+</sup>(+)-ATPase. *Proc. Natl. Acad. Sci. U. S. A* **87**, 2466-2470 (1990).
120. Putney,J.W., Jr. A model for receptor-regulated calcium entry. *Cell Calcium* **7**, 1-12 (1986).
121. Parekh,A.B. & Putney,J.W., Jr. Store-operated calcium channels. *Physiol Rev.* **85**, 757-810 (2005).
122. Frise,E., Knoblich,J.A., Younger-Shepherd,S., Jan,L.Y., & Jan,Y.N. The *Drosophila* Numb protein inhibits signaling of the Notch receptor during cell-cell

- interaction in sensory organ lineage. *Proc. Natl. Acad. Sci. U. S. A* **93**, 11925-11932 (1996).
123. Bani-Yaghoub, M. *et al.* A switch in numb isoforms is a critical step in cortical development. *Dev. Dyn.* **236**, 696-705 (2007).
  124. Artavanis-Tsakonas, S. Alagille syndrome--a notch up for the Notch receptor. *Nat. Genet.* **16**, 212-213 (1997).
  125. Del, M.G., Grego-Bessa, J., Gonzalez-Rajal, A., Bolos, V., & de la Pompa, J.L. Monitoring Notch1 activity in development: evidence for a feedback regulatory loop. *Dev. Dyn.* **236**, 2594-2614 (2007).
  126. Kopan, R. & Ilagan, M.X. Gamma-secretase: proteasome of the membrane? *Nat. Rev. Mol. Cell Biol.* **5**, 499-504 (2004).
  127. Sisodia, S.S. & St George-Hyslop, P.H. gamma-Secretase, Notch, Abeta and Alzheimer's disease: where do the presenilins fit in? *Nat. Rev. Neurosci.* **3**, 281-290 (2002).
  128. Fiuza, U.M. & Arias, A.M. Cell and molecular biology of Notch. *J. Endocrinol.* **194**, 459-474 (2007).
  129. Ma, H.T. *et al.* Requirement of the inositol trisphosphate receptor for activation of store-operated Ca<sup>2+</sup> channels. *Science* **287**, 1647-1651 (2000).
  130. Ma, H.T. *et al.* Modification of phospholipase C-gamma-induced Ca<sup>2+</sup> signal generation by 2-aminoethoxydiphenyl borate. *Biochem. J.* **376**, 667-676 (2003).
  131. Clapham, D.E. TRP channels as cellular sensors. *Nature* **426**, 517-524 (2003).
  132. Nilius, B. Store-operated Ca<sup>2+</sup> entry channels: still elusive! *Sci. STKE.* **2004**, e36 (2004).
  133. Voccoli, V., Mazzoni, F., Garcia-Gil, M., & Colombaioni, L. Serum-withdrawal-dependent apoptosis of hippocampal neuroblasts involves Ca<sup>++</sup> release by endoplasmic reticulum and caspase-12 activation. *Brain Res.* **1147**, 1-11 (2007).
  134. Yao, Y., Ferrer-Montiel, A.V., Montal, M., & Tsien, R.Y. Activation of store-operated Ca<sup>2+</sup> current in *Xenopus* oocytes requires SNAP-25 but not a diffusible messenger. *Cell* **98**, 475-485 (1999).
  135. Patterson, R.L., van Rossum, D.B., & Gill, D.L. Store-operated Ca<sup>2+</sup> entry: evidence for a secretion-like coupling model. *Cell* **98**, 487-499 (1999).



136. Cayouette,S., Lussier,M.P., Mathieu,E.L., Bousquet,S.M., & Boulay,G. Exocytotic Insertion of TRPC6 Channel into the Plasma Membrane upon Gq Protein-coupled Receptor Activation. *J. Biol. Chem.* **279**, 7241-7246 (2004).
137. Clapham,D.E. TRP channels as cellular sensors. *Nature* **426**, 517-524 (2003).
138. Montell,C. The TRP superfamily of cation channels. *Sci. STKE.* **2005**, re3 (2005).
139. Soboloff,J. *et al.* Role of endogenous TRPC6 channels in Ca<sup>2+</sup> signal generation in A7r5 smooth muscle cells. *J. Biol. Chem.* **280**, 39786-39794 (2005).
140. Tully,K. & Treistman,S.N. Distinct Intracellular Calcium Profiles Following Influx Through N- Versus L-Type Calcium Channels: Role of Ca<sup>2+</sup>-Induced Ca<sup>2+</sup> Release. *J Neurophysiol* **92**, 135-143 (2004).
141. Guo,M., Jan,L.Y., & Jan,Y.N. Control of daughter cell fates during asymmetric division: interaction of Numb and Notch. *Neuron* **17**, 27-41 (1996).
142. Uemura,T., Shepherd,S., Ackerman,L., Jan,L.Y., & Jan,Y.N. numb, a gene required in determination of cell fate during sensory organ formation in Drosophila embryos. *Cell* **58**, 349-360 (1989).
143. Wakamatsu,Y., Maynard,T.M., Jones,S.U., & Weston,J.A. NUMB localizes in the basal cortex of mitotic avian neuroepithelial cells and modulates neuronal differentiation by binding to NOTCH-1. *Neuron* **23**, 71-81 (1999).
144. Kimble,J. & Simpson,P. The LIN-12/Notch signaling pathway and its regulation. *Annu. Rev. Cell Dev. Biol.* **13**, 333-361 (1997).
145. Arumugam,T.V. *et al.* Gamma secretase-mediated Notch signaling worsens brain damage and functional outcome in ischemic stroke. *Nat. Med.* **12**, 621-623 (2006).
146. Jaekel,R. & Klein,T. The Drosophila Notch inhibitor and tumor suppressor gene lethal (2) giant discs encodes a conserved regulator of endosomal trafficking. *Dev. Cell* **11**, 655-669 (2006).
147. Kaether,C., Haass,C., & Steiner,H. Assembly, trafficking and function of gamma-secretase. *Neurodegener. Dis.* **3**, 275-283 (2006).